Haus, Hermann A., and James R. Melcher. *Electromagnetic Fields and Energy.* Englewood Cliffs, NJ: Prentice-Hall, 1989. ISBN: 9780132490207.

10

MAGNETOQUASISTATIC RELAXATION AND DIFFUSION

10.0 INTRODUCTION

In the MQS approximation, Ampère's law relates the magnetic field intensity $\mathbf{H}$ to the current density $\mathbf{J}$.

$$\boxed{\nabla \times \mathbf{H} = \mathbf{J}} \tag{1}$$

Augmented by the requirement that $\mathbf{H}$ have no divergence, this law was the theme of Chap. 8. Two types of physical situations were considered. Either the current density was imposed, or it existed in perfect conductors. In both cases, we were able to determine $\mathbf{H}$ without being concerned about the details of the electric field distribution.

In Chap. 9, the effects of magnetizable materials were represented by the magnetization density $\mathbf{M}$, and the magnetic flux density, defined as $\mathbf{B} \equiv \mu_o(\mathbf{H}+\mathbf{M})$, was found to have no divergence.

$$\boxed{\nabla \cdot \mathbf{B} = 0} \tag{2}$$

Provided that $\mathbf{M}$ is either given or instantaneously determined by $\mathbf{H}$ (as was the case throughout most of Chap. 9), and that $\mathbf{J}$ is either given or subsumed by the boundary conditions on perfect conductors, these two magnetoquasistatic laws determine $\mathbf{H}$ throughout the volume.

In this chapter, our first objective will be to determine the distribution of $\mathbf{E}$ around perfect conductors. Then we shall broaden our physical domain to include finite conductors, especially in situations where currents are caused by an $\mathbf{E}$ that

is induced by the time rate of change of $\mathbf{B}$. In both cases, we make explicit use of Faraday's law.

$$\boxed{\nabla \times \mathbf{E} = -\frac{\partial \mathbf{B}}{\partial t}} \tag{3}$$

In the EQS systems considered in Chaps. 4–7, the curl of $\mathbf{H}$ generated by the time rate of change of the displacement flux density was not of interest. Ampère's law was adequately incorporated by the continuity law. However, in MQS systems, the curl of $\mathbf{E}$ generated by the magnetic induction on the right in (1) is often of primary importance. We had fields that depended on time rates of change in Chap. 7.

We have already seen the consequences of Faraday's law in Sec. 8.4, where MQS systems of perfect conductors were considered. The electric field intensity $\mathbf{E}$ inside a perfect conductor must be zero, and hence $\mathbf{B}$ has to vanish inside the perfect conductor if $\mathbf{B}$ varies with time. This leads to $\mathbf{n} \cdot \mathbf{B} = 0$ on the surface of a perfect conductor. Currents induced in the surface of perfect conductors assure the proper discontinuity of $\mathbf{n} \times \mathbf{H}$ from a finite value outside to zero inside.

Faraday's law was in evidence in Sec. 8.4 and accounted for the voltage at terminals connected to each other by perfect conductors. Faraday's law makes it possible to have a voltage at terminals connected to each other by a perfect "short." A simple experiment brings out some of the subtlety of the voltage definition in MQS systems. Its description is followed by an overview of the chapter.

Demonstration 10.0.1. Nonuniqueness of Voltage in an MQS System

A magnetic flux is created in the toroidal magnetizable core shown in Fig. 10.0.1 by driving the winding with a sinsuoidal current. Because it is highly permeable (a ferrite), the core guides a magnetic flux density $\mathbf{B}$ that is much greater than that in the surrounding air.

Looped in series around the core are two resistors of unequal value, $R_1 \neq R_2$. Thus, the terminals of these resistors are connected together to form a pair of "nodes." One of these nodes is grounded. The other is connected to high-impedance voltmeters through two leads that follow the different paths shown in Fig. 10.0.1. A dual-trace oscilloscope is convenient for displaying the voltages.

The voltages observed with the leads connected to the same node not only differ in magnitude but are 180 degrees out of phase.

Faraday's integral law explains what is observed. A cross-section of the core, showing the pair of resistors and voltmeter leads, is shown in Fig. 10.0.2. The scope resistances are very large compared to R_1 and R_2, so the current carried by the voltmeter leads is negligible. This means that if there is a current i through one of the series resistors, it must be the same as that through the other.

The contour C_c follows the closed circuit formed by the series resistors. Faraday's integral law is now applied to this contour. The flux passing through the surface S_c spanning C_c is defined as Φ_λ. Thus,

$$\oint_{C_1} \mathbf{E} \cdot d\mathbf{s} = -\frac{d\Phi_\lambda}{dt} = i(R_1 + R_2) \tag{4}$$

where

$$\Phi_\lambda \equiv \int_{S_c} \mathbf{B} \cdot d\mathbf{a} \tag{5}$$

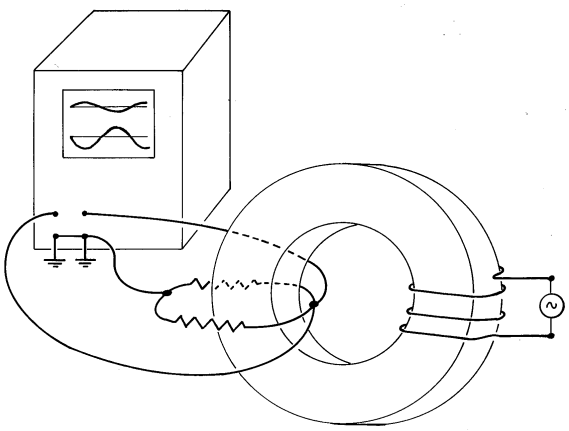

Fig. 10.0.1 A pair of unequal resistors are connected in series around a magnetic circuit. Voltages measured between the terminals of the resistors by connecting the nodes to the dual-trace oscilloscope, as shown, differ in magnitude and are 180 degrees out of phase.

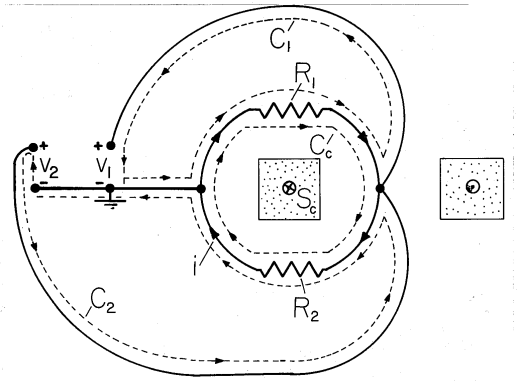

Fig. 10.0.2 Schematic of circuit for experiment of Fig. 10.0.1, showing contours used with Faraday's law to predict the differing voltages v_1 and v_2.

Given the magnetic flux, (4) can be solved for the current i that must circulate around the loop formed by the resistors.

To determine the measured voltages, the same integral law is applied to contours C_1 and C_2 of Fig. 10.0.2. The surfaces spanning the contours link a negligible flux density, so the circulation of $\mathbf{E}$ around these contours must vanish.

$$\oint_{C_1} \mathbf{E} \cdot d\mathbf{s} = v_1 + iR_1 = 0 \tag{6}$$

$$\oint_{C_2} \mathbf{E} \cdot d\mathbf{s} = -v_2 + iR_2 = 0 \tag{7}$$

The observed voltages are found by solving (4) for i, which is then substituted into (6) and (7).

$$v_1 = \frac{R_1}{R_1 + R_2} \frac{d\Phi_\lambda}{dt} \tag{8}$$

$$v_2 = -\frac{R_2}{R_1 + R_2} \frac{d\Phi_\lambda}{dt} \tag{9}$$

From this result it follows that

$$\frac{v_1}{v_2} = -\frac{R_1}{R_2} \tag{10}$$

Indeed, the voltages not only differ in magnitude but are of opposite signs.

Suppose that one of the voltmeter leads is disconnected from the right node, looped through the core, and connected directly to the grounded terminal of the same voltmeter. The situation is even more remarkable because we now have a voltage at the terminals of a "short." However, it is also more familiar. We recognize from Sec. 8.4 that the measured voltage is simply $d\lambda/dt$, where the flux linkage is in this case Φ_λ.

In Sec. 10.1, we begin by investigating the electric field in the free space regions of systems of perfect conductors. Here the viewpoint taken in Sec. 8.4 has made it possible to determine the distribution of **B** without having to determine **E** in the process. The magnetic induction appearing on the right in Faraday's law, (1), is therefore known, and hence the law prescribes the curl of **E**. From the introduction to Chap. 8, we know that this is not enough to uniquely prescribe the electric field. Information about the divergence of **E** must also be given, and this brings into play the electrical properties of the materials filling the regions between the perfect conductors.

The analyses of Chaps. 8 and 9 determined **H** in two special situations. In one case, the current distribution was prescribed; in the other case, the currents were flowing in the surfaces of perfect conductors. To see the more general situation in perspective, we may think of MQS systems as analogous to networks composed of inductors and resistors, such as shown in Fig. 10.0.3. In the extreme case where the source is a rapidly varying function of time, the inductors alone determine the currents. Finding the current distribution in this "high frequency" limit is analogous to finding the **H**-field, and hence the distribution of surface currents, in the systems of perfect conductors considered in Sec. 8.4. Finding the electric field in perfectly conducting systems, the objective in Sec. 10.1 of this chapter, is analogous to determining the distribution of voltage in the circuit in the limit where the inductors dominate.

In the opposite extreme, if the driving voltage is slowly varying, the inductors behave as shorts and the current distribution is determined by the resistive network alone. In terms of fields, the response to slowly varying sources of current is essentially the steady current distribution described in the first half of Chap. 7. Once this distribution of **J** has been determined, the associated magnetic field can be found using the superposition integrals of Chap. 8.

In Secs. 10.2–10.4, we combine the MQS laws of Chap. 8 with those of Faraday and Ohm to describe the evolution of **J** and **H** when neither of these limiting cases prevails. We shall see that the field response to a step of excitation goes from a

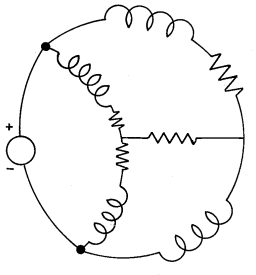

Fig. 10.0.3 Magnetoquasistatic systems with Ohmic conductors are generalizations of inductor-resistor networks. The steady current distribution is determined by the resistors, while the high-frequency response is governed by the inductors.

distribution governed by the perfect conductivity model just after the step is applied (the circuit dominated by the inductors), to one governed by the steady conduction laws for $\mathbf{J}$, and Biot-Savart for $\mathbf{H}$ after a long time (the circuit dominated by the resistors with the flux linkages then found from $\lambda = Li$). Under what circumstances is the perfectly conducting model appropriate? The characteristic times for this magnetic field diffusion process will provide the answer.

10.1 MAGNETOQUASISTATIC ELECTRIC FIELDS IN SYSTEMS OF PERFECT CONDUCTORS

The distribution of $\mathbf{E}$ around the conductors in MQS systems is of engineering interest. For example, the amount of insulation required between conductors in a transformer is dependent on the electric field.

In systems composed of perfect conductors and free space, the distribution of magnetic field intensity is determined by requiring that $\mathbf{n} \cdot \mathbf{B} = 0$ on the perfectly conducting boundaries. Although this condition is required to make the electric field tangential to the perfect conductor vanish, as we saw in Sec. 8.4, it is not necessary to explicitly refer to $\mathbf{E}$ in finding $\mathbf{H}$. Thus, in Faraday's law of induction, (10.0.3), the right-hand side is known. The source of *curl* $\mathbf{E}$ is thus known. To determine the source of *div* $\mathbf{E}$, further information is required.

The regions outside the perfect conductors, where $\mathbf{E}$ is to be found, are presumably filled with relatively insulating materials. To identify the additional information necessary for the specification of $\mathbf{E}$, we must be clear about the nature of these materials. There are three possibilities:

- Although the material is much less conducting than the adjacent "perfect" conductors, the charge relaxation time is far shorter than the times of interest. Thus, $\partial\rho/\partial t$ is negligible in the charge conservation equation and, as a result, the current density is solenoidal. Note that this is the situation in the MQS approximation. In the following discussion, we will then presume that if this situation prevails, the region is filled with a material of *uniform* conductivity, in which case $\mathbf{E}$ is solenoidal within the material volume. (Of course, there

may be surface charges on the boundaries.)

$$\nabla \cdot \mathbf{E} = 0 \tag{1}$$

- The second situation is typical when the "perfect" conductors are surrounded by materials commonly used to insulate wires. The charge relaxation time is generally much longer than the times of interest. Thus, no unpaired charges can flow into these "insulators" and they remain charge free. Provided they are of uniform permittivity, the E field is again solenoidal within these materials.
- If the charge relaxation time is on the same order as times characterizing the currents carried by the conductors, then the distribution of unpaired charge is governed by the combination of Ohm's law, charge conservation, and Gauss' law, as discussed in Sec. 7.7. If the material is not only of uniform conductivity but of uniform permittivity as well, this charge density is zero in the volume of the material. It follows from Gauss' law that $\mathbf{E}$ is once again solenoidal in the material volume. Of course, surface charges may exist at material interfaces.

The electric field intensity is broken into particular and homogeneous parts

$$\mathbf{E} = \mathbf{E}_p + \mathbf{E}_h \tag{2}$$

where, in accordance with Faraday's law, (10.0.3), and (1),

$$\nabla \times \mathbf{E}_p = -\frac{\partial \mathbf{B}}{\partial t} \tag{3}$$

$$\nabla \cdot \mathbf{E}_p = 0 \tag{4}$$

and

$$\nabla \times \mathbf{E}_h = 0 \tag{5}$$

$$\nabla \cdot \mathbf{E}_h = 0. \tag{6}$$

Our approach is reminiscent of that taken in Chap. 8, where the roles of $\mathbf{E}$ and $\partial\mathbf{B}/\partial t$ are respectively taken by $\mathbf{H}$ and $-\mathbf{J}$. Indeed, if all else fails, the particular solution can be generated by using an adaptation of the Biot-Savart law, (8.2.7).

$$\mathbf{E}_p = -\frac{1}{4\pi}\int_{V'} \frac{\frac{\partial \mathbf{B}}{\partial t}(\mathbf{r}') \times \mathbf{i}_{\mathbf{r}'\mathbf{r}}}{|\mathbf{r} - \mathbf{r}'|^2} dv' \tag{7}$$

Given a particular solution to (3) and (4), the boundary condition that there be no tangential $\mathbf{E}$ on the surfaces of the perfect conductors is satisfied by finding a solution to (5) and (6) such that

$$\mathbf{n} \times \mathbf{E} = 0 \Rightarrow \mathbf{n} \times \mathbf{E}_h = -\mathbf{n} \times \mathbf{E}_p \tag{8}$$

on those surfaces.

Given the particular solution, the boundary value problem has been reduced to one familiar from Chap. 5. To satisfy (5), we let $\mathbf{E}_h = -\nabla\Phi$. It then follows from (6) that Φ satisfies Laplace's equation.

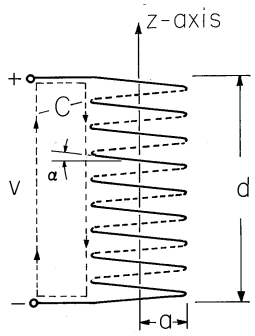

Fig. 10.1.1 Side view of long inductor having radius a and length d.

Example 10.1.1. Electric Field around a Long Coil

What is the electric field distribution in and around a typical inductor? An approximate analysis for a coil of many turns brings out the reason why transformer and generator designers often speak of the "volts per turn" that must be withstood by insulation. The analysis illustrates the concept of breaking the solution into a particular rotational field and a homogeneous conservative field.

Consider the idealized coil of Fig. 10.1.1. It is composed of a thin, perfectly conducting wire, wound in a helix of length d and radius a. The magnetic field can be found by approximating the current by a surface current $\mathbf{K}$ that is ϕ directed about the z axis of a cylindrical coodinate system having the z axis coincident with the axis of the coil. For an N-turn coil, this surface current density is $K_\phi = Ni/d$. If the coil is very long, $d \gg a$, the magnetic field produced within is approximately uniform

$$H_z = \frac{Ni}{d} \tag{9}$$

while that outside is essentially zero (Example 8.2.1). Note that the surface current density is just that required to terminate $\mathbf{H}$ in accordance with Ampère's continuity condition.

With such a simple magnetic field, a particular solution is easily obtained. We recognize that the perfectly conducting coil is on a natural coordinate surface in the cylindrical coordinate system. Thus, we write the z component of (3) in cylindrical coordinates and look for a solution to $\mathbf{E}$ that is independent of ϕ. The solution resulting from an integration over r is

$$\mathbf{E}_p = \mathbf{i}_\phi \begin{cases} -\frac{\mu_o r}{2}\frac{dH_z}{dt} & r < a \\ -\frac{\mu_o a^2}{2r}\frac{dH_z}{dt} & r > a \end{cases} \tag{10}$$

Because there is no magnetic field outside the coil, the outside solution for $\mathbf{E_p}$ is irrotational.

If we adhere to the idealization of the wire as an inclined current sheet, the electric field along the wire in the sheet must be zero. The particular solution does not satisfy this condition, and so we now must find an irrotational and solenoidal $\mathbf{E_h}$ that cancels the component of $\mathbf{E_p}$ tangential to the wire.

A section of the wire is shown in Fig. 10.1.2. What axial field E_z must be added to that given by (10) to make the net $\mathbf{E}$ perpendicular to the wire? If E_z and E_ϕ are to be components of a vector normal to the wire, then their ratio must be

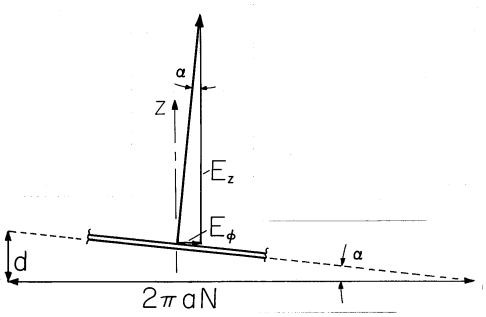

Fig. 10.1.2 With the wire from the inductor of Fig. 10.1.1 stretched into a straight line, it is evident that the slope of the wire in the inductor is essentially the total length of the coil, d, divided by the total length of the wire, $2\pi aN$.

the same as the ratio of the total length of the wire to the length of the coil.

$$\frac{E_z}{E_\phi} = \frac{2\pi aN}{d}; \qquad r = a \tag{11}$$

Using (9) and (10) at $r = a$, we have

$$E_z = -\frac{\mu_o \pi a^2 N^2}{d^2}\frac{di}{dt} \tag{12}$$

The homogeneous solution possesses this field E_z on the surface of the cylinder of radius a and length d. This field determines the potential Φ_h over the surface (within an arbitrary constant). Since $\nabla^2\Phi_h = 0$ everywhere in space and the tangential E_h field prescribes Φ_h on the cylinder, Φ_h is uniquely determined everywhere within an additive constant. Hence, the conservative part of the field is determined everywhere.

The voltage between the terminals is determined from the line integral of $\mathbf{E} \cdot d\mathbf{s}$ between the terminals. The field of the particular solution is ϕ-directed and gives no contribution. The entire contribution to the line integral comes from the homogeneous solution (12) and is

$$v = -E_z d = \frac{\mu_o N^2 \pi a^2}{d}\frac{di}{dt} \tag{13}$$

Note that this expression takes the form Ldi/dt, where the inductance L is in agreement with that found using a contour coincident with the wire, (8.4.18).

We could think of the terminal voltage as the sum of N "voltages per turn" $E_z d/N$. If we admit to the finite size of the wires, the electric stress between the wires is essentially this "voltage per turn" divided by the distance between wires.

The next example identifies the particular and homogeneous solutions in a somewhat more formal fashion.

Example 10.1.2. Electric Field of a One-Turn Solenoid

The cross-section of a one-turn solenoid is shown in Fig. 10.1.3. It consists of a circular cylindrical conductor having an inside radius a much less than its length in

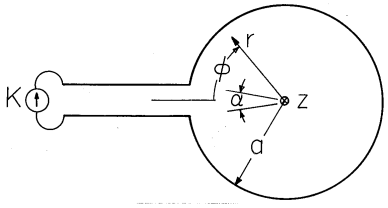

Fig. 10.1.3 A one-turn solenoid of infinite length is driven by the distributed source of current density, $K(t)$.

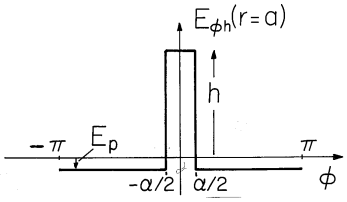

Fig. 10.1.4 Tangential component of homogeneous electric field at $r = a$ in the configuration of Fig. 10.1.3.

the z direction. It is driven by a distributed current source $K(t)$ through the plane parallel plates to the left. This current enters through the upper sheet conductor, circulates in the ϕ direction around the one turn, and leaves through the lower plate. The spacing between these plates is small compared to a.

As in the previous example, the field inside the solenoid is uniform, axial, and equal to the surface current

$$\mathbf{H} = \mathbf{i_z} K(t) \tag{14}$$

and a particular solution can be found by applying Faraday's integral law to a contour having the arbitrary radius $r < a$, (10).

$$\mathbf{E}_p = E_{\phi p}\mathbf{i}_\phi; \qquad E_{\phi p} \equiv -\frac{\mu_o r}{2}\frac{dK}{dt} \tag{15}$$

This field clearly does not satisfy the boundary condition at $r = a$, where it has a tangential value over almost all of the surface. The homogeneous solution must have a tangential component that cancels this one. However, this field must also be conservative, so its integral around the circumference at $r = a$ must be zero. Thus, the plot of the ϕ component of the homogeneous solution at $r = a$, shown in Fig. 10.1.4, has no average value. The amplitude of the tall rectangle is adjusted so that the net area under the two functions is zero.

$$E_{\phi p}(2\pi - \alpha) = h\alpha \Rightarrow h = E_{\phi p}\Big(\frac{2\pi}{\alpha} - 1\Big) \tag{16}$$

The field between the edges of the input electrodes is approximated as being uniform right out to the contacts with the solenoid.

We now find a solution to Laplace's equation that matches this boundary condition on the tangential component of $\mathbf{E}$. Because E_ϕ is an even function of ϕ, Φ is taken as an odd function. The origin is included in the region of interest, so the polar coordinate solutions (Table 5.7.1) take the form

$$\Phi = \sum_{n=1}^{\infty} A_n r^n \sin n\phi \tag{17}$$

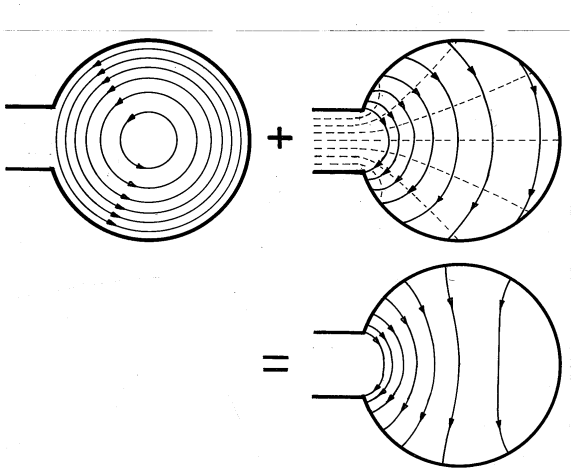

Fig. 10.1.5 Graphical representation of solution for the electric field in the configuration of Fig. 10.1.3.

It follows that

$$E_{\phi h} = -\frac{1}{r}\frac{\partial \Phi}{\partial \phi} = -\sum_{n=1}^{\infty} nA_n r^{n-1}\cos n\phi. \tag{18}$$

The coefficients A_n are evaluated, as in Sec. 5.5, by multiplying both sides of this expression by $\cos(m\phi)$ and integrating from $\phi = -\pi$ to $\phi = \pi$.

$$\begin{aligned}\int_{-\pi}^{-\alpha/2} -E_{\phi p}\cos m\phi d\phi + \int_{-\alpha/2}^{\alpha/2} E_{\phi p}\left(\frac{2\pi}{\alpha} - 1\right)\cos m\phi d\phi \\ + \int_{\alpha/2}^{\pi} -E_{\phi p}\cos m\phi d\phi = -mA_m a^{m-1}\pi\end{aligned} \tag{19}$$

Thus, the coefficients needed to evaluate the potential of (17) are

$$A_m = -\frac{4E_{\phi p}(r=a)}{m^2 a^{m-1}\alpha}\sin\frac{m\alpha}{2} \tag{20}$$

Finally, the desired field intensity is the sum of the particular solution, (15), and the homogeneous solution, the gradient of (17).

$$\begin{aligned}\mathbf{E} = -\frac{\mu_o a}{2}\frac{dK}{dt}\left[\frac{r}{a}\mathbf{i}_\phi + 4\sum_{n=1}^{\infty}\frac{\sin\frac{n\alpha}{2}}{\alpha n}\left(\frac{r}{a}\right)^{n-1}\cos n\phi\mathbf{i}_\phi\right. \\ \left. + 4\sum_{n=1}^{\infty}\frac{\sin\frac{n\alpha}{2}}{n\alpha}\left(\frac{r}{a}\right)^{n-1}\sin n\phi\mathbf{i}_\mathbf{r}\right]\end{aligned} \tag{21}$$

The superposition of fields represented in this solution is shown graphically in Fig. 10.1.5. A conservative field is added to the rotational field. The former has

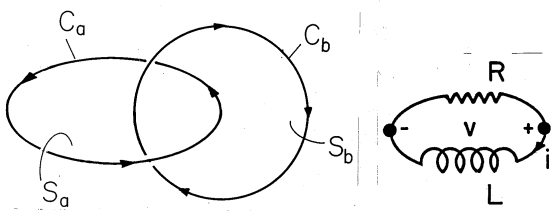

Fig. 10.2.1 Current induced in accordance with Faraday's law circulates on contour C_a. Through Ampère's law, it results in magnetic field that follows contour C_b.

a potential at $r = a$ that is a linearly increasing function of ϕ between the input electrodes, increasing from a negative value at the lower electrode at $\phi = -\alpha/2$, passing through zero at the midplane, and reaching an equal positive value at the upper electrode at $\phi = \alpha/2$. The potential decreases in a linear fashion from this high as ϕ is increased, again passing through zero at $\phi = 180$ degrees, and reaching the negative value upon returning to the lower input electrode. Equipotential lines therefore join points on the solenoid periphery with points at the same potential between the input electrodes. Note that the electric field associated with this potential indeed has the tangential component required to cancel that from the rotational part of the field, the proof of this being in the last of the plots.

Often the vector potential provides conveniently a particular solution. With **B** replaced by $\nabla \times \mathbf{A}$,

$$\nabla \times \left(\mathbf{E} + \frac{\partial \mathbf{A}}{\partial t} \right) = 0 \tag{22}$$

Suppose **A** has been determined. Then the quantity in parantheses must be equal to the gradient of a potential Φ so that

$$\mathbf{E} = -\frac{\partial \mathbf{A}}{\partial t} - \nabla \Phi \tag{23}$$

In the examples treated, the first term in this expression is the particular solution, while the second is the homogeneous solution.

10.2 NATURE OF FIELDS INDUCED IN FINITE CONDUCTORS

If a conductor is situated in a time-varying magnetic field, the induced electric field gives rise to currents. From Sec. 8.4, we have shown that these currents prevent the penetration of the magnetic field into a perfect conductor. How high must σ be to treat a conductor as perfect? In the next two sections, we use specific analytical models to answer this question. Here we preface these developments with a discussion of the interplay between the laws of Faraday, Ampère and Ohm that determines the distribution, duration, and magnitude of currents in conductors of finite conductivity.

The integral form of Faraday's law, applied to the surface S_a and contour C_a of Fig. 10.2.1, is

$$\oint_{C_a} \mathbf{E} \cdot d\mathbf{s} = -\frac{d}{dt} \int_{S_a} \mathbf{B} \cdot d\mathbf{a} \tag{1}$$

Ohm's law, $\mathbf{J} = \sigma\mathbf{E}$, introduced into (1), relates the current density circulating around a tube following C_a to the enclosed magnetic flux.

$$\oint_{C_a} \frac{\mathbf{J}}{\sigma} \cdot d\mathbf{s} = -\frac{d}{dt}\int_{S_a} \mathbf{B} \cdot d\mathbf{a} \tag{2}$$

This statement applies to every circulating current "hose" in a conductor. Let us concentrate on one such hose. The current flows parallel to the hose, and therefore $\mathbf{J} \cdot d\mathbf{s} = Jds$. Suppose that the cross-sectional area of the hose is $A(s)$. Then $JA(s) = i$, the current in the hose, and

$$\oint \frac{A(s)}{\sigma} ds = R \tag{3}$$

is the resistance of the hose. Therefore,

$$iR = -\frac{d\lambda}{dt} \tag{4}$$

Equation (2) describes how the time-varying magnetic flux gives rise to a circulating current. Ampère's law states how that current, in turn, produces a magnetic field.

$$\oint_{C_b} \mathbf{H} \cdot d\mathbf{s} = \int_{S_b} \mathbf{J} \cdot d\mathbf{a} \tag{5}$$

Typically, that field circulates around a contour such as C_b in Fig. 10.2.1, which is pierced by $\mathbf{J}$. With Gauss' law for $\mathbf{B}$, Ampère's law provides the relation for $\mathbf{H}$ produced by $\mathbf{J}$. This information is summarized by the "lumped circuit" relation

$$\lambda = Li \tag{6}$$

The combination of (4) and (6) provides a differential equation for the circuit current $i(t)$. The equivalent circuit for the differential equation is the series interconnection of a resistor R with an inductor L, as shown in Fig. 10.2.1. The solution is an exponentially decaying function of time with the time constant L/R.

The combination of (2) and (5)– of the laws of Faraday, Ampère, and Ohm– determine $\mathbf{J}$ and $\mathbf{H}$. The field problem corresponds to a continuum of "circuits." We shall find that the time dependence of the fields is governed by time constants having the nature of L/R. This time constant will be of the form

$$\tau_m = \mu\sigma l_1 l_2 \tag{7}$$

In contrast with the charge relaxation time ϵ/σ of EQS, this *magnetic diffusion time* depends on the product of two characteristic lengths, denoted here by l_1 and l_2. For given time rates of change and electrical conductivity, the larger the system, the more likely it is to behave as a perfect conductor.

Although we will not use the integral laws to determine the fields in the finite conductivity systems of the next sections, they are often used to make engineering

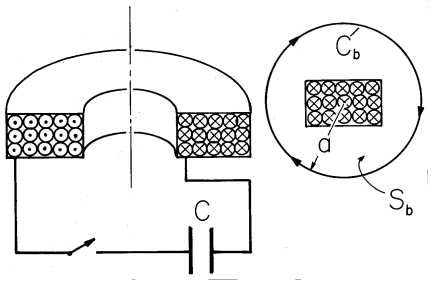

Fig. 10.2.2 When the spark gap switch is closed, the capacitor discharges into the coil. The contour C_b is used to estimate the average magnetic field intensity that results.

approximations. The following demonstration is quantified using rough approximations in a style that typifies how field theory is often applied to practical problems.

Demonstration 10.2.1. Edgerton's Boomer

The capacitor in Fig. 10.2.2, $C = 25\mu F$, is initially charged to $v = 4kV$. The spark gap switch is then closed so that the capacitor can discharge into the 50-turn coil. This demonstration has been seen by many visitors to Prof. Harold Edgerton's Strobe Laboratory at M.I.T.

Given that the average radius of a coil winding $a = 7$ cm, and that the height of the coil is also on the order of a, roughly what magnetic field is generated? Ampère's integral law, (5), can be applied to the contour C_b of the figure to obtain an approximate relation between the average $\mathbf{H}$, which we will call H_1, and the coil current i_1.

$$H_1 \approx \frac{N_1 i_1}{2\pi a} \tag{8}$$

To determine i_1, we need the inductance L_{11} of the coil. To this end, the flux linkage of the coil is approximated by N_1 times the product of the average coil area and the average flux density.

$$\lambda \approx N_1(\pi a^2)\mu_o H_1 \tag{9}$$

From these last two equations, one obtains $\lambda = L_{11} i_1$, where the inductance is

$$L_{11} \approx \frac{\mu_o a N_1^2}{2} \tag{10}$$

Evaluation gives $L_{11} = 0.1$ mH.

With the assumption that the combined resistance of the coil, switch, and connecting leads is small enough so that the voltage across the capacitor and the current in the inductor oscillate at the frequency

$$\omega = \frac{1}{\sqrt{CL_{11}}} \tag{11}$$

we can determine the peak current by recognizing that the energy $\frac{1}{2}Cv^2$ initially stored in the capacitor is one quarter of a cycle later stored in the inductor.

$$\frac{1}{2}L_{11}i_p^2 \approx \frac{1}{2}Cv_p^2 \Rightarrow i_p = v_p\sqrt{C/L_{11}} \tag{12}$$

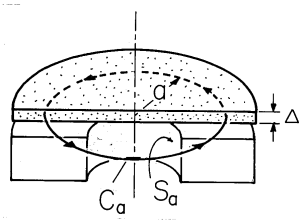

Fig. 10.2.3 Metal disk placed on top of coil shown in Fig. 10.2.2.

Thus, the peak current in the coil is $i_1 = 2,000A$. We know both the capacitance and the inductance, so we can also determine the frequency with which the current oscillates. Evaluation gives $\omega = 20 \times 10^3 s^{-1}$ ($f = 3$kHz).

The H field oscillates with this frequency and has an amplitude given by evaluating (8). We find that the peak field intensity is $H_1 = 2.3 \times 10^5$ A/m so that the peak flux density is 0.3 T (3000 gauss).

Now suppose that a conducting disk is placed just above the driver coil as shown in Fig. 10.2.3. What is the current induced in the disk? Choose a contour that encloses a surface S_a which links the upward-directed magnetic flux generated at the center of the driver coil. With E defined as an average azimuthally directed electric field in the disk, Faraday's law applied to the contour bounding the surface S_a gives

$$2\pi a E_\phi = -\frac{d}{dt}\int_{S_a} \mathbf{B}\cdot d\mathbf{a} \approx -\frac{d}{dt}(\mu_o H_1 \pi a^2) \tag{13}$$

The average current density circulating in the disk is given by Ohm's law.

$$J_\phi = \sigma E_\phi = -\frac{\sigma \mu_o a}{2}\frac{dH_1}{dt} \tag{14}$$

If one were to replace the disk with his hand, what current density would he feel? To determine the peak current, the derivative is replaced by ωH_1. For the hand, $\sigma \approx 1$ S/m and (14) gives 20 mA/cm^2. This is more than enough to provide a "shock."

The conductivity of an aluminum disk is much larger, namely 3.5×10^7 S/m. According to (14), the current density should be 35 million times larger than that in a human hand. However, we need to remind ourselves that in using Ampère's law to determine the driving field, we have ignored contributions due to the induced current in the disk.

Ampère's integral law can also be used to approximate the field induced by the current in the disk. Applied to a contour that loops around the current circulating in the disk rather than in the driving coil, (2) requires that

$$H_{ind} \approx \frac{i_2}{2\pi a} \approx \frac{\Delta a J_\phi}{2\pi a} \tag{15}$$

Here, the cross-sectional area of the disk through which the current circulates is approximated by the product of the disk thickness Δ and the average radius a.

It follows from (14) and (15) that the induced field gets to be on the order of the imposed field when

$$\frac{H_{ind}}{H_1} \approx \frac{\Delta \sigma \mu_o a}{4\pi}\frac{1}{|H_1|}\left|\frac{dH_1}{dt}\right| \approx \frac{\tau_m}{4\pi}\omega \tag{16}$$

where

$$\tau_m \equiv \mu_o \sigma \Delta a \tag{17}$$

Note that τ_m takes the form of (7), where $l_1 = \Delta$ and $l_2 = a$.

For an aluminum disk of thickness $\Delta = 2$ mm, $a = 7$ cm, $\tau_m = 6$ ms, so $\omega\tau_m/4\pi \approx 10$, and the field associated with the induced current is comparable to that imposed by the driving coil.[1] The surface of the disk is therefore one where $\mathbf{n} \cdot \mathbf{B} \approx 0$. The lines of magnetic flux density passing upward through the center of the driving coil are trapped between the driver coil and the disk as they turn radially outward. These lines are sketched in Fig. 10.2.4.

In the terminology introduced with Example 9.7.4, the disk is the secondary of a transformer. In fact, τ_m is the time constant L_{22}/R of the secondary, where L_{22} and R are the inductance and resistance of a circuit representing the disk. Indeed, the condition for ideal transformer operation, (9.7.26), is equivalent to having $\omega\tau_m/4\pi \gg 1$. The windings in power transformers are subject to the forces we now demonstrate.

If an aluminum disk is placed on the coil and the switch closed, a number of applications emerge. First, there is a bang, correctly suggesting that the disk can be used as an acoustic transducer. Typical applications are to deep-sea acoustic sounding. The force density $\mathbf{F}(N/m^3)$ responsible for this sound follows from the Lorentz law (Sec. 11.9)

$$\mathbf{F} = \mathbf{J} \times \mu_o \mathbf{H} \tag{18}$$

Note that regardless of the polarity of the driving current, and hence of the average $\mathbf{H}$, this force density acts upward. It is a force of repulsion. With the current distribution in the disk represented by a surface current density K, and $\mathbf{B}$ taken as one half its average value (the factor of 1/2 will be explained in Example 11.9.3), the total upward force on the disk is

$$\mathbf{f} = \int_V \mathbf{J} \times \mathbf{B} dV \approx \frac{1}{2} KB(\pi a^2)\mathbf{i_z} \tag{19}$$

By Ampère's law, the surface current K in the disk is equal to the field in the region between the disk and the driver, and hence essentially equal to the average H. Thus, with an additional factor of $\frac{1}{2}$ to account for time averaging the sinusoidally varying drive, (19) becomes

$$f \approx f_o \equiv \frac{1}{4}\mu_o H^2(\pi a^2) \tag{20}$$

In evaluating this expression, the value of $\mathbf{H}$ adjacent to the disk with the disk resting on the coil is required. As suggested by Fig. 10.2.4, this field intensity is larger than that given by (8). Suppose that the field is intensified in the gap between coil and plate by a factor of about 2 so that $H \simeq 5 \times 10^5 A$. Then, evaluation of (20) gives $10^3 N$ or more than 1000 times the force of gravity on an $80g$ aluminum disk. How high would the disk fly? To get a rough idea, it is helpful to know that the driver current decays in several cycles. Thus, the average driving force is essentially an impulse, perhaps as pictured in Fig. 10.2.5 having the amplitude of (20) and a duration $T = 1$ ms. With the aerodynamic drag ignored, Newton's law requires that

$$M\frac{dV}{dt} = f_o T u_o(t) \tag{21}$$

[1] As we shall see in the next sections, because the calculation is not self-consistent, the inequality $\omega\tau_m \gg 1$ indicates that the induced field is comparable to and not in excess of the one imposed.

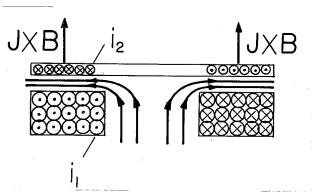

Fig. 10.2.4 Currents induced in the metal disk tend to induce a field that bucks out that imposed by the driving coil. These currents result in a force on the disk that tends to propel it upward.

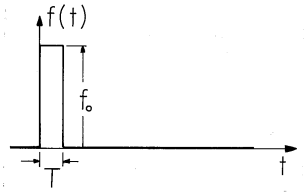

Fig. 10.2.5 Because the magnetic force on the disk is always positive and lasts for a time T shorter than the time it takes the disk to leave the vicinity of the coil, it is represented by an impulse of magnitude f_oT.

where $M = 0.08kg$ is the disk mass, V is its velocity, and $u_o(t)$ is the unit impulse. Integration of this expression from $t = 0^-$ (when the velocity $V = 0$) to $t = 0^+$ gives

$$MV(O^+) = f_oT \tag{22}$$

For the numbers we have developed, this initial velocity is about 10 m/s or about 20 miles/hr. Perhaps of more interest is the height h to which the disk would be expected to travel. If we require that the initial kinetic energy $\frac{1}{2}MV^2$ be equal to the final potential energy Mgh ($g = 9.8$ m/s^2), this height is $\frac{1}{2}V^2/g \simeq 5$ m.

The voltage and capacitance used here for illustration are modest. Even so, if the disk is thin and malleable, it is easily deformed by the field. Metal forming and transport are natural applications of this phenomenon.

10.3 DIFFUSION OF AXIAL MAGNETIC FIELDS THROUGH THIN CONDUCTORS

This and the next section are concerned with the influence of thin-sheet conductors of finite conductivity on distributions of magnetic field. The demonstration of the previous section is typical of physical situations of interest. By virtue of Faraday's law, an applied field induces currents in the conducting sheet. Through Ampère's law, these in turn result in an induced field tending to buck out the imposed field. The resulting field has a time dependence reflecting not only that of the applied field but the conductivity and dimensions of the conductor as well. This is the subject of the next two sections.

A class of configurations with remarkably simple fields involves one or more sheet conductors in the shape of cylinders of infinite length. As illustrated in Fig.

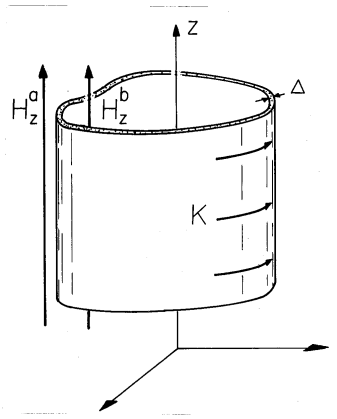

Fig. 10.3.1 A thin shell having conductivity σ and thickness Δ has the shape of a cylinder of arbitrary cross-section. The surface current density $K(t)$ circulates in the shell in a direction perpendicular to the magnetic field, which is parallel to the cylinder axis.

10.3.1, these are uniform in the z direction but have an arbitrary cross-sectional geometry. In this section, the fields are z directed and the currents circulate around the z axis through the thin sheet. Fields and currents are pictured as independent of z.

The current density **J** is divergence free. If we picture the current density as flowing in planes perpendicular to the z axis, and as essentially uniform over the thickness Δ of the sheet, then the surface current density must be independent of the azimuthal position in the sheet.

$$K = K(t) \tag{1}$$

Ampère's continuity condition, (9.5.3), requires that the adjacent axial fields are related to this surface current density by

$$\boxed{-H_z^a + H_z^b = K} \tag{2}$$

In a system with a single cylinder, with a given circulating surface current density K and insulating materials of uniform properties both outside (a) and inside (b), a uniform axial field inside and no field outside is the exact solution to Ampère's law and the flux continuity condition. (We saw this in Demonstration 8.2.1 and in Example 8.4.2. for a solenoid of circular cross-section.) In a system consisting of nested cylinders, each having an arbitrary cross-sectional geometry and each carrying its own surface current density, the magnetic fields between cylinders would be uniform. Then (2) would relate the uniform fields to either side of any given sheet.

In general, K is not known. To relate it to the axial field, we must introduce the laws of Ohm and Faraday. The fact that K is uniform makes it possible to exploit the integral form of the latter law, applied to a contour C that circulates through the cylinder.

$$\oint_C \mathbf{E} \cdot d\mathbf{s} = -\frac{d}{dt} \int_S \mathbf{B} \cdot d\mathbf{a} \tag{3}$$

To replace $\mathbf{E}$ in this expression, we multiply $\mathbf{J} = \sigma\mathbf{E}$ by the thickness Δ to relate the surface current density to E, the magnitude of $\mathbf{E}$ inside the sheet.

$$K \equiv \Delta J = \Delta\sigma E \Rightarrow E = \frac{K}{\Delta\sigma} \tag{4}$$

If Δ and σ are uniform, then E (like K), is the same everywhere along the sheet. However, either the thickness or the conductivity could be functions of azimuthal position. If σ and Δ are given, the integral on the left in (3) can be taken, since K is constant. With s denoting the distance along the contour C, (3) and (4) become

$$\boxed{K \oint_C \frac{ds}{\Delta(s)\sigma(s)} = -\frac{d}{dt}\int_S \mathbf{B}\cdot d\mathbf{a}} \tag{5}$$

Of most interest is the case where the thickness and conductivity are uniform and (5) becomes

$$\frac{KP}{\Delta\sigma} = -\frac{d}{dt}\int_S \mathbf{B}\cdot d\mathbf{a} \tag{6}$$

with P denoting the peripheral length of the cylinder.

The following are examples based on this model.

Example 10.3.1. Diffusion of Axial Field into a Circular Tube

The conducting sheet shown in Fig. 10.3.2 has the shape of a long pipe with a wall of uniform thickness and conductivity. There is a uniform magnetic field $\mathbf{H} = \mathbf{i_z}H_o(t)$ in the space outside the tube, perhaps imposed by means of a coaxial solenoid. What current density circulates in the conductor and what is the axial field intensity H_i inside?

Representing Ohm's law and Faraday's law of induction, (6) becomes

$$\frac{K}{\Delta\sigma}2\pi a = -\frac{d}{dt}(\mu_o\pi a^2 H_i) \tag{7}$$

Ampère's law, represented by the continuity condition, (2), requires that

$$K = -H_o + H_i \tag{8}$$

In these two expressions, H_o is a given driving field, so they can be combined into a single differential equation for either K or H_i. Choosing the latter, we obtain

$$\frac{dH_i}{dt} + \frac{H_i}{\tau_m} = \frac{H_o}{\tau_m} \tag{9}$$

where

$$\tau_m = \frac{1}{2}\mu_o\sigma\Delta a \tag{10}$$

This expression pertains regardless of the driving field. In particular, suppose that before $t = 0$, the fields and surface current are zero, and that when $t = 0$, the outside H_o is suddenly turned on. The appropriate solution to (9) is the combination

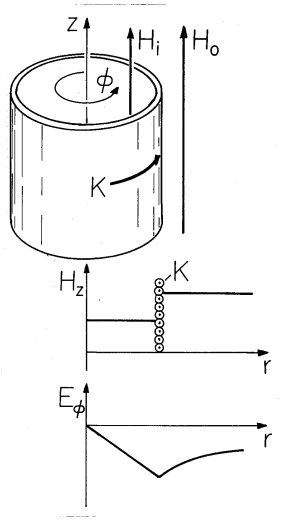

Fig. 10.3.2 Circular cylindrical conducting shell with external axial field intensity $H_o(t)$ imposed. The response to a step in applied field is a current density that initially shields the field from the inner region. As this current decays, the field penetrates into the interior and is finally uniform throughout.

of the particular solution $H_i = H_o$ and the homogeneous solution $\exp(-t/\tau_m)$ that satisfies the initial condition.

$$H_i = H_o(1 - e^{-t/\tau_m}) \tag{11}$$

It follows from (8) that the associated surface current density is

$$K = -H_o e^{-t/\tau_m} \tag{12}$$

At a given instant, the axial field has the radial distribution shown in Fig. 10.3.2b. Outside, the field is imposed to be equal to H_o, while inside it is at first zero but then fills in with an exponential dependence on time. After a time that is long compared to τ_m, the field is uniform throughout. Implied by the discontinuity in field intensity at $r = a$ is a surface current density that initially terminates the outside field. When $t = 0$, $K = -H_o$, and this results in a field that bucks out the field imposed on the inside region. The decay of this current, expressed by (12), accounts for the penetration of the field into the interior region.

This example illustrates what one means by "perfect conductor approximation." A perfect conductor would shield out the magnetic field forever. A physical conductor shields it out for times $t \ll \tau_m$. Thus, in the MQS approximation, a conductor can be treated as perfect for times that are short compared with the characteristic time τ_m. The electric field $E_\phi \equiv E$ is given by applying (3) to a contour having an arbitrary radius r.

$$2\pi r E = -\frac{d}{dt}(\mu_o H_i \pi r^2) \Rightarrow E = -\frac{\mu_o r}{2}\frac{dH_i}{dt} \qquad r < a \tag{13}$$

$$\begin{aligned} 2\pi r E &= -\frac{d}{dt}(\mu_o H_i \pi a^2) - \frac{d}{dt}[\mu_o H_o \pi (r^2 - a^2)] \Rightarrow \\ E &= -\frac{\mu_o a}{2}\left[\frac{a}{r}\frac{dH_i}{dt} + \left(\frac{r}{a} - \frac{a}{r}\right)\frac{dH_o}{dt}\right] \qquad r > a \end{aligned} \tag{14}$$

At $r = a$, this particular solution matches that already found using the same integral law in the conductor. In this simple case, it is not necessary to match boundary conditions by superimposing a homogeneous solution taking the form of a conservative field.

We consider next an example where the electric field is not simply the particular solution.

Example 10.3.2. Diffusion into Tube of Nonuniform Conductivity

Once again, consider the circular cylindrical shell of Fig. 10.3.2 subject to an imposed axial field $H_o(t)$. However, now the conductivity is a function of azimuthal position.

$$\sigma = \frac{\sigma_o}{1 + \alpha \cos \phi} \tag{15}$$

The integral in (5), resulting from Faraday's law, becomes

$$K \oint_C \frac{ds}{\Delta(s)\sigma(s)} = \frac{K}{\Delta\sigma_o} \int_0^{2\pi} (1 + \alpha \cos \phi) a d\phi = \frac{2\pi a}{\Delta\sigma_o} K \tag{16}$$

and hence

$$\frac{2\pi a}{\Delta\sigma_o} K = -\frac{d}{dt}(\pi a^2 \mu_o H_i) \tag{17}$$

Ampère's continuity condition, (2), once again becomes

$$K = -H_o + H_i \tag{18}$$

Thus, H_i is determined by the same expressions as in the previous example, except that σ is replaced by σ_o. The surface current response to a step in imposed field is again the exponential of (12).

It is the electric field distribution that is changed. Using (15), (4) gives

$$E = \frac{K}{\Delta\sigma_o}(1 + \alpha \cos \phi) \tag{19}$$

for the electric field inside the conductor. The E field in the adjacent free space regions is found using the familiar approach of Sec. 10.1. The particular solution is the same as for the uniformly conducting shell, (13) and (14). To this we add a homogeneous solution $\mathbf{E}_h = -\nabla\Phi$ such that the sum matches the tangential field given by (19) at $r = a$. The ϕ-independent part of (19) is already matched by the particular solution, and so the boundary condition on the homogeneous part requires that

$$-\frac{1}{a}\frac{\partial \Phi}{\partial \phi}(r = a) = \frac{K\alpha}{\Delta\sigma_o} \cos \phi \Rightarrow \Phi(r = a) = -\frac{K\alpha a}{\Delta\sigma_o} \sin \phi \tag{20}$$

Solutions to Laplace's equation that vary as $\sin(\phi)$ match this condition. Outside, the appropriate r dependence is $1/r$ while inside it is r. With the coefficients of these potentials adjusted to match the boundary condition given by (20), it follows that the electric field outside and inside the shell is

$$\mathbf{E} = \begin{cases} -\frac{\mu_o r}{2}\frac{dH_i}{dt}\mathbf{i}_\phi - \nabla\Phi_i & r < a \\ -\frac{\mu_o a}{2}\left[\frac{a}{r}\frac{dH_i}{dt} + \left(\frac{r}{a} - \frac{a}{r}\right)\frac{dH_o}{dt}\right]\mathbf{i}_\phi - \nabla\Phi_o & a < r \end{cases} \tag{21}$$

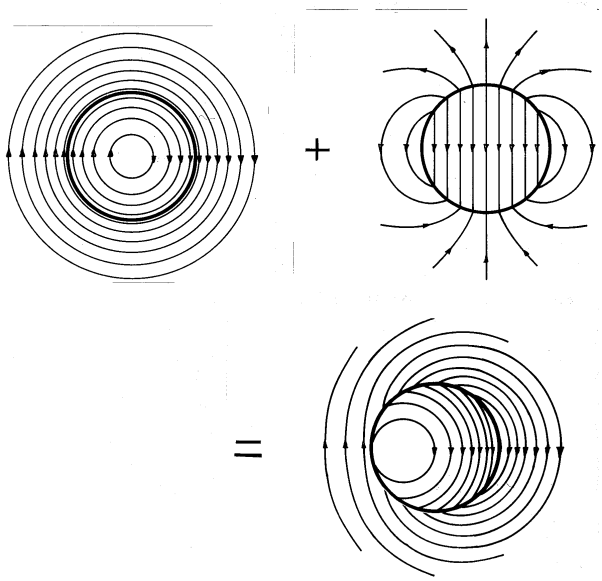

Fig. 10.3.3 Electric field induced in regions inside and outside shell (having conductivity that varies with azimuthal position) portrayed as the sum of a particular rotational and homogeneous conservative solution. Conductivity is low on the right and high on the left, $\alpha = 0.5$.

where

$$\Phi_i = -\frac{K\alpha}{\Delta\sigma_o} r \sin\phi \tag{22}$$

$$\Phi_o = -\frac{K\alpha a^2}{\Delta\sigma_o} \frac{\sin\phi}{r} \tag{23}$$

These expressions can be evaluated using (11) and (12) for H_i and K for the electric field associated with a step in applied field. It follows that **E**, like the surface current and the induced **H**, decays exponentially with the time constant of (10). At a given instant, the distribution of **E** is as illustrated in Fig. 10.3.3. The total solution is the sum of the particular rotational and homogeneous conservative parts. The degree to which the latter influences the total field depends on α, which reflects the inhomogeneity in conductivity.

For positive α, the conductivity is low on the right (when $\phi = 0$) and high on the left in Fig. 10.3.3. In accordance with (7.2.8), positive unpaired charge is induced in the transition region where the current flows from high to low conductivity, and negative charge is induced in the transition region from low to high conductivity. The field of the homogeneous solution shown in the figure originates and terminates on the induced charges.

We shall return to models based on conducting cylindrical shells in axial fields. Systems of conducting shells can be used to represent the nonuniform flow of current in thick conductors. The model will also be found useful in determining the rate of induction heating for cylindrical objects.

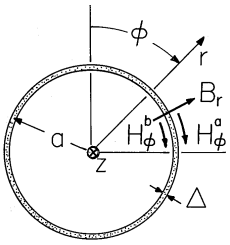

Fig. 10.4.1 Cross-section of circular cylindrical conducting shell having its axis perpendicular to the magnetic field.

10.4 DIFFUSION OF TRANSVERSE MAGNETIC FIELDS THROUGH THIN CONDUCTORS

In this section we study magnetic induction of currents in thin conducting shells by fields transverse to the shells. In Sec. 10.3, the magnetic fields were automatically tangential to the conductor surfaces, so we did not have the opportunity to explore the limitations of the boundary condition $\mathbf{n} \cdot \mathbf{B} = 0$ used to describe a "perfect conductor." In this section the imposed fields generally have components normal to the conducting surface.

The steps we now follow can be applied to many different geometries. We specifically consider the circular cylindrical shell shown in cross-section in Fig. 10.4.1. It has a length in the z direction that is very large compared to its radius a. Its conductivity is σ, and it has a thickness Δ that is much less than its radius a. The regions outside and inside are specified by (a) and (b), respectively.

The fields to be described are directed in planes perpendicular to the z axis and do not depend on z. The shell currents are z directed. A current that is directed in the $+z$ direction at one location on the shell is returned in the $-z$ direction at another. The closure for this current circulation can be imagined to be provided by perfectly conducting endplates, or by a distortion of the current paths from the z direction near the cylinder ends (end effect).

The shell is assumed to have essentially the same permeability as free space. It therefore has no tendency to guide the magnetic flux density. Integration of the *magnetic flux continuity* condition over an incremental volume enclosing a section of the shell shows that the normal component of $\mathbf{B}$ is continuous through the shell.

$$\mathbf{n} \cdot (\mathbf{B}^a - \mathbf{B}^b) = 0 \Rightarrow B_r^a = B_r^b \tag{1}$$

Ohm's law relates the axial current density to the axial electric field, $J_z = \sigma E_z$. This density is presumed to be essentially uniformly distributed over the radial cross-section of the shell. Multiplication of both sides of this expression by the thickness Δ of the shell gives an expression for the surface current density in the shell.

$$K_z \equiv \Delta J_z = \Delta \sigma E_z \tag{2}$$

Faraday's law is a vector equation. Of the three components, the radial one is dominant in describing how the time-varying magnetic field induces electric fields, and hence currents, tangential to the shell. In writing this component, we assume that the fields are independent of z.

$$\frac{1}{a}\frac{\partial E_z}{\partial \phi} = -\frac{\partial B_r}{\partial t} \tag{3}$$

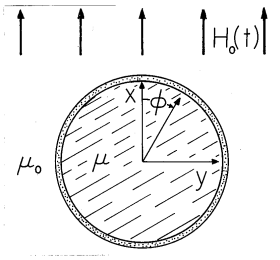

Fig. 10.4.2 Circular cylindrical conducting shell filled by insulating material of permeability μ and surrounded by free space. A magnetic field $H_o(t)$ that is uniform at infinity is imposed transverse to the cylinder axis.

Ampère's continuity condition makes it possible to express the surface current density in terms of the tangential fields to either side of the shell.

$$K_z = H_\phi^a - H_\phi^b \tag{4}$$

These last three expressions are now combined to obtain the desired continuity condition.

$$\boxed{\frac{1}{\Delta\sigma a}\frac{\partial}{\partial\phi}(H_\phi^a - H_\phi^b) = -\frac{\partial B_r}{\partial t}} \tag{5}$$

Thus, the description of the shell is encapsulated in the two continuity conditions, (1) and (5).

The thin-shell model will now be used to place in perspective the idealized boundary condition of perfect conductivity. In the following example, the conductor is subjected to a field that is suddenly turned on. The field evolution with time places in review the perfect conductivity mode of MQS systems in Chap. 8 and the magnetization phenomena of Chap. 9. Just after the field is turned on, the shell acts like the perfect conductors of Chap. 8. As time goes on, the shell currents decay to zero and only the magnetization of Chap. 9 persists.

Example 10.4.1. Diffusion of Transverse Field into Circular Cylindrical Conducting Shell with a Permeable Core

A permeable circular cylindrical core having radius a is shown in Fig. 10.4.2. It is surrounded by a thin conducting shell, having thickness Δ and conductivity σ. A uniform time-varying magnetic field intensity $H_o(t)$ is imposed transverse to the axis of the shell and core. The configuration is long enough in the axial direction to justify representing the fields as independent of the axial coordinate z.

Reflecting the fact that the region outside (o) is free space while that inside (i) is the material of linear permeability are the constitutive laws

$$\mathbf{B}^o = \mu_o\mathbf{H}^o; \qquad \mathbf{B}^i = \mu\mathbf{H}^i \tag{6}$$

For the two-dimensional fields in the $r-\phi$ plane, where the sheet current is in the z direction, the scalar potential provides a convenient description of the field.

$$\mathbf{H} = -\nabla\Psi \tag{7}$$

We begin by recognizing the form taken by Ψ far from the cylinder.

$$\Psi = -H_o r \cos\phi \tag{8}$$

Note that substitution of this relation into (7) indeed gives the uniform imposed field.

Given the ϕ dependence of (8), we assume solutions of the form

$$\Psi^o = -H_o r \cos\phi + A\frac{\cos\phi}{r} \tag{9}$$

$$\Psi^i = Cr\cos\phi$$

where A and C are coefficients to be determined by the continuity conditions. In preparation for the evaluation of these conditions, the assumed solutions are substituted into (7) to give the flux densities

$$\mathbf{B}^o = \mu_o\big(H_o + \frac{A}{r^2}\big)\cos\phi\mathbf{i}_\mathbf{r} - \mu_o\big(H_o - \frac{A}{r^2}\big)\sin\phi\mathbf{i}_\phi \tag{10}$$

$$\mathbf{B}^i = -\mu C(\cos\mathbf{i}_\mathbf{r} - \sin\phi\mathbf{i}_\phi)$$

Should we expect that these functions can be used to satisfy the continuity conditions at $r = a$ given by (1) and (5) at every azimuthal position ϕ? The inside and outside radial fields have the same ϕ dependence, so we are assured of being able to adjust the two coefficients to satisfy the flux continuity condition. Moreover, in evaluating (5), the ϕ derivative of H_ϕ has the same ϕ dependence as B_r. Thus, satisfying the continuity conditions is assured.

The first of two relations between the coefficients and H_o follows from substituting (10) into (1).

$$\mu_o\big(H_o + \frac{A}{a^2}\big) = -\mu C \tag{11}$$

The second results from a similar substitution into (5).

$$-\frac{1}{\Delta\sigma a}\big(H_o - \frac{A}{a^2}\big) - \frac{C}{\Delta\sigma a} = -\mu_o\left(\frac{dH_o}{dt} + \frac{1}{a^2}\frac{dA}{dt}\right) \tag{12}$$

With C eliminated from this latter equation by means of (11), we obtain an ordinary differential equation for $A(t)$.

$$\frac{dA}{dt} + \frac{A}{\tau_m} = -a^2\frac{dH_o}{dt} + \frac{H_o a}{\mu_o\Delta\sigma}\big(1 - \frac{\mu_o}{\mu}\big) \tag{13}$$

The time constant τ_m takes the form of (10.2.7).

$$\tau_m = \mu_o\sigma\Delta a\big(\frac{\mu}{\mu + \mu_o}\big) \tag{14}$$

In (13), the time dependence of the imposed field is arbitrary. The form of this expression is the same as that of (7.9.28), so techniques for dealing with initial conditions and for determining the sinusoidal steady state response introduced there are directly applicable here.

Response to a Step in Applied Field. Suppose there is no field inside or outside the conducting shell before $t = 0$ and that H_o is a step function of magnitude H_m turned on when $t = 0$. With D a coefficient determined by the initial condition, the solution to (13) is the sum of a particular and a homogeneous solution.

$$A = H_m a^2 \frac{(\mu - \mu_o)}{(\mu + \mu_o)} + De^{-t/\tau_m} \tag{15}$$

Integration of (13) from $t = 0^-$ to $t = 0^+$ shows that $A(0) = -H_m a^2$, so that D is evaluated and (15) becomes

$$A = H_m a^2 \left[\frac{(\mu - \mu_o)}{(\mu + \mu_o)} (1 - e^{-t/\tau_m}) - e^{-t/\tau_m} \right] \tag{16}$$

This expression makes it possible to evaluate C using (11). Finally, these coefficients are substituted into (9) to give the potential outside and inside the shell.

$$\Psi^o = -H_m a \left\{ \frac{r}{a} - \frac{a}{r} \left[\frac{(\mu - \mu_o)}{(\mu + \mu_o)} (1 - e^{-t/\tau_m}) - e^{-t/\tau_m} \right] \right\} \cos\phi \tag{17}$$

$$\Psi^i = -H_m a \frac{r}{a} \frac{2\mu_o}{(\mu + \mu_o)} (1 - e^{-t/\tau_m}) \cos\phi \tag{18}$$

The field evolution represented by these expressions is shown in Fig. 10.4.3, where lines of $\mathbf{B}$ are portrayed. When the transverse field is suddenly turned on, currents circulate in the shell in such a direction as to induce a field that bucks out the one imposed. For an applied field that is positive, this requires that the surface current be in the $-z$ direction on the right and returned in the $+z$ direction on the left. This surface current density can be analytically expressed first by using (10) to evaluate Ampère's continuity condition

$$K_z = H_\phi^o - H_\phi^i = \left[-H_o \left(1 - \frac{\mu_o}{\mu} \right) + \frac{A}{a^2} \left(1 + \frac{\mu_o}{\mu} \right) \right] \sin\phi \tag{19}$$

and then by using (15).

$$K_z = -2H_m e^{-t/\tau_m} \sin\phi \tag{20}$$

With the decay of K_z, the external field goes from that for a perfect conductor (where $\mathbf{n} \cdot \mathbf{B} = 0$) to the field that would have been found if there were no conducting shell. The magnetizable core tends to draw this field into the cylinder.

The coefficient A represents the amplitude of a two-dimensional dipole that has a field equivalent to that of the shell current. Just after the field is applied, A is negative and hence the equivalent dipole moment is directed opposite to the imposed field. This results in a field that is diverted around the shell. With the passage of time, this dipole moment can switch sign. This sign reversal occurs only if $\mu > \mu_o$, making it clear that it is due to the magnetization of the core. In the absence of the core, the final field is uniform.

Under what conditions can the shell be regarded as perfectly conducting? The answer involves not only σ but also the time scale and the size, and to some extent,

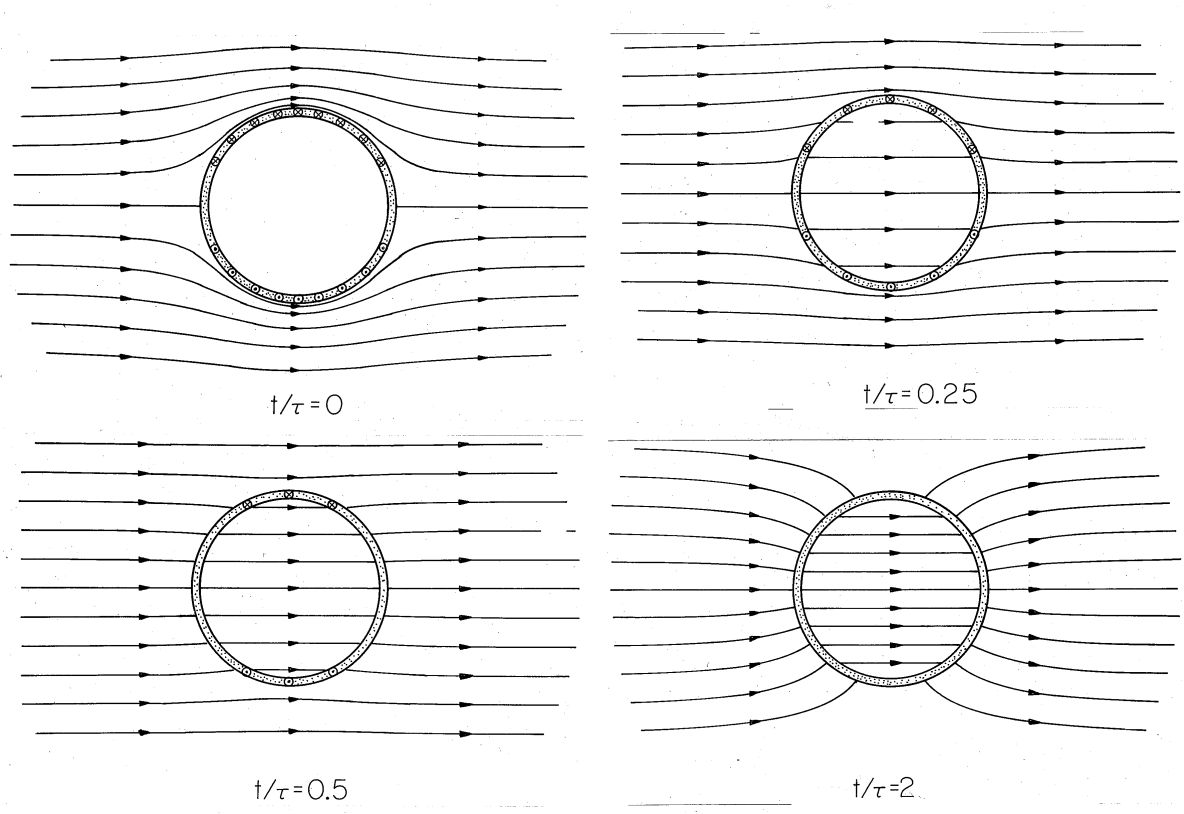

Fig. 10.4.3 When $t = 0$, a magnetic field that is uniform at infinity is suddenly imposed on the circular cylindrical conducting shell. The cylinder is filled by an insulating material of permeability $\mu = 200\mu_o$. When $t/\tau = 0$, an instant after the field is applied, the surface currents completely shield the field from the central region. As time goes on, these currents decay, until finally the field is no longer influenced by the conducting shell. The final field is essentially perpendicular to the highly permeable core. In the absence of this core, the final field would be uniform.

the permeability. For our step response, the shell shields out the field for times that are short compared to τ_m, as given by (14).

Demonstration 10.4.1. Currents Induced in a Conducting Shell

The apparatus of Demonstration 10.2.1 can be used to make evident the shell currents predicted in the previous example. A cylinder of aluminum foil is placed on the driver coil, as shown in Fig. 10.4.4. With the discharge of the capacitor through the coil, the shell is subjected to an abruptly applied field. By contrast with the step function assumed in the example, this field oscillates and decays in a few cycles. However, the reversal of the field results in a reversal in the induced shell current, so regardless of the time dependence of the driving field, the force density $\mathbf{J} \times \mathbf{B}$ is in the same direction.

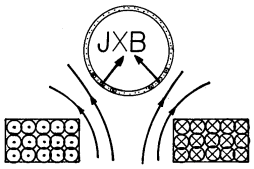

Fig. 10.4.4 In an experiment giving evidence of the currents induced when a field is suddenly applied transverse to a conducting cylinder, an aluminum foil cylinder, subjected to the field produced by the experiment of Fig. 10.2.2, is crushed.

The force associated with the induced current is inward. If the applied field were truly uniform, the shell would then be "squashed" inward from the right and left by the field. Because the field is not really uniform, the cylinder of foil is observed to be compressed inward more at the bottom than at the top, as suggested by the force vectors drawn in Fig. 10.4.4. Remember that the postulated currents require paths at the ends of the cylinder through which they can circulate. In a roll of aluminum foil, these return paths are through the shell walls in those end regions that extend beyond the region of the applied field.

The derivation of the continuity conditions for a circular cylindrical shell follows a format that is applicable to other geometries. Examples are a planar sheet and a spherical shell.

10.5 MAGNETIC DIFFUSION LAWS

The self-consistent evolution of the magnetic field intensity $\mathbf{H}$ with its source $\mathbf{J}$ induced in Ohmic materials of finite conductivity is familiar from the previous two sections. In the models so far considered, the induced currents were in thin conducting shells. Thus, in the processes of magnetic relaxation described in these sections, the currents were confined to thin regions that could be represented by dynamic continuity conditions.

In this and the next two sections, the conductor extends throughout at least part of a volume of interest. Like $\mathbf{H}$, the current density in Ampère's law

$$\nabla \times \mathbf{H} = \mathbf{J} \tag{1}$$

is an unknown function. For an Ohmic material, it is proportional to the local electric field intensity.

$$\mathbf{J} = \sigma \mathbf{E} \tag{2}$$

In turn, $\mathbf{E}$ is induced in accordance with Faraday's law

$$\nabla \times \mathbf{E} = -\frac{\partial \mu \mathbf{H}}{\partial t} \tag{3}$$

The conductor is presumed to have uniform conductivity σ and permeability μ. For linear magnetization, the magnetic flux continuity law is

$$\nabla \cdot \mu \mathbf{H} = 0 \tag{4}$$

In the MQS approximation the current density **J** is also solenoidal, as can be seen by taking the divergence of Ampère's law.

$$\nabla \cdot \mathbf{J} = 0 \tag{5}$$

In the previous two sections, we combined the continuity conditions implied by (1) and (4) with the other laws to obtain dynamic continuity conditions representing thin conducting sheets. The regions between sheets were insulating, and so the field distributions in these regions were determined by solving Laplace's equation. Here we combine the differential laws to obtain a new differential equation that takes on the role of Laplace's equation in determining the distribution of magnetic field intensity.

If we solve Ohm's law, (2), for **E** and substitute for **E** in Faraday's law, we have in one statement the link between magnetic induction and induced current density.

$$\nabla \times \left(\frac{\mathbf{J}}{\sigma} \right) = -\frac{\partial \mu \mathbf{H}}{\partial t} \tag{6}$$

The current density is eliminated from this expression by using Ampère's law, (1). The result is an expression of **H** alone.

$$\nabla \times \left(\frac{\nabla \times \mathbf{H}}{\sigma} \right) = -\frac{\partial \mu \mathbf{H}}{\partial t} \tag{7}$$

This expression assumes a somewhat more familiar appearance when σ and μ are constants, so that they can be taken outside the operations. Further, it follows from (4) that **H** is solenoidal so the use of a vector identity[2] turns (7) into

$$\boxed{\frac{1}{\mu\sigma} \nabla^2 \mathbf{H} = \frac{\partial \mathbf{H}}{\partial t}} \tag{8}$$

At each point in a material having uniform conductivity and permeability, the magnetic field intensity satisfies this vector form of the *diffusion equation*. The distribution of current density implied by the **H** found by solving this equation with appropriate boundary conditions follows from Ampère's law, (1).

Physical Interpretation. With the understanding that **H** and **J** are solenoidal, the derivation of (8) identifies the feedback between source and field that underlies the magnetic diffusion process. The effect of the (time-varying) field on the source embodied in the combined laws of Faraday and Ohm, (6), is perhaps best appreciated by integrating (6) over any fixed open surface S enclosed by a contour C. By Stokes' theorem, the integration of the curl over the surface transforms into an integration around the enclosing contour. Thus, (6) implies that

$$-\oint_C \frac{\mathbf{J}}{\sigma} \cdot d\mathbf{s} = \frac{d}{dt} \int_S \mu \mathbf{H} \cdot d\mathbf{a} \tag{9}$$

[2] $\nabla \times \nabla \times \mathbf{H} = \nabla(\nabla \cdot \mathbf{H}) - \nabla^2 \mathbf{H}$

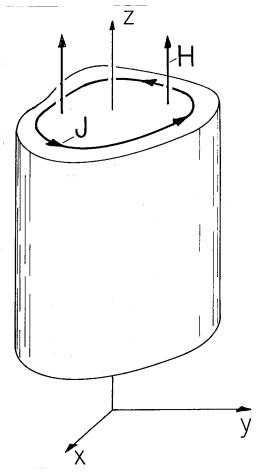

Fig. 10.5.1 Configurations in which cylindrically shaped conductors having axes parallel to the magnetic field have currents transverse to the field in $x-y$ planes.

and requires that the electromotive force around *any* closed path must be equal to the time rate of change of the enclosed magnetic flux. Numerical approaches to solving magnetic diffusion problems may in fact approximate a system by a finite number of circuits, each representing a current tube with its own resistance and flux linkage. To represent the return effect of the current on **H**, the diffusion equation also incorporates Ampère's law, (1).

The relaxation of axial fields through thin shells, developed in Sec. 10.3, is an example where the geometry of the conductor and the symmetry make the current tubes described by (9) readily discernible. The diffusion of an axial magnetic field H_z into the volume of cylindrically shaped conductors, as shown in Fig. 10.5.1, is a generalization of the class of axial problems described in Sec. 10.3. As the only component of **H**, $H_z(x, y)$ must satisfy (8).

$$\frac{1}{\mu\sigma}\nabla^2 H_z = \frac{\partial H_z}{\partial t} \tag{10}$$

The current density is then directed transverse to this field and given in terms of H_z by Ampère's law.

$$\mathbf{J} = \mathbf{i_x}\frac{\partial H_z}{\partial y} - \mathbf{i_y}\frac{\partial H_z}{\partial x} \tag{11}$$

Thus, the current density circulates in $x - y$ planes.

Methods for solving the diffusion equation are natural extensions of those used in previous chapters for dealing with Laplace's equation. Although we confine ourselves in the next two sections to diffusion in one spatial dimension, the thin-shell models give an intuitive impression as to what can be expected as magnetic fields diffuse into solid conductors having a wide range of geometries.

Consider the coaxial thin shells shown in Fig. 10.5.2 as a model for a solid cylindrical conductor. Following the approach outlined in Sec. 10.3, suppose that the exterior field H_o is an imposed function of time. Then the fields between sheets (H_1

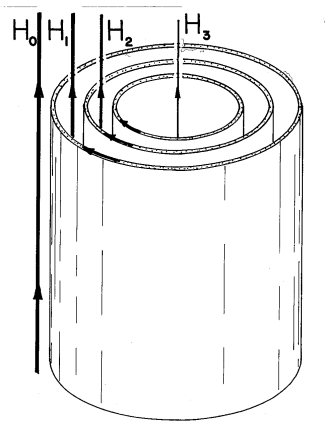

Fig. 10.5.2 Example of an axial field configuration composed of coaxial conducting shells of infinite axial length. When an exterior field H_o is applied, currents circulating in the shells tend to shield out the imposed field.

and H_2) and in the central region (H_3) are determined by a system of three ordinary differential equations having $H_o(t)$ as a drive. Associated with the evolution of these fields are surface currents in the shells that tend to shield the field from the region within. In the limit where the number of shells is infinite, the field distribution in a solid conductor could be represented by such coupled thin shells. However, the more practical approach used in the next sections is to solve the diffusion equation exactly. The situations considered are in cartesian rather than polar coordinates.

10.6 MAGNETIC DIFFUSION TRANSIENT RESPONSE

The self-consistent distribution of current density and magnetic field intensity in the volume of a uniformly conducting material is determined from the laws given in Sec. 10.5 and summarized by the magnetic diffusion equation (10.5.8). In this section, we illustrate magnetic diffusion phenomena by considering the transient that results when a current is abruptly turned on or off.

In contrast to Laplace's equation, the diffusion equation involves a time rate of change, and so it is necessary to deal with the time dependence in much the same way as the space dependence. The diffusion process considered in this section is in one spatial dimension, with time as the second "dimension." Our approach builds on product solutions and the solution of boundary value problems by superposition, as introduced in Chap. 5.

The class of configurations of interest is illustrated in Fig. 10.6.1. Perfectly conducting electrodes are driven along their edges at $x = -b$ by a distributed current source. The uniformly conducting material is sandwiched between these electrodes. The current originating in the source then circulates in the x direction through the electrode in the $y = 0$ plane to a point where it passes in the y direction through the conducting material. It is then returned to the source through the other perfectly conducting plate. Note that this configuration is a special case of

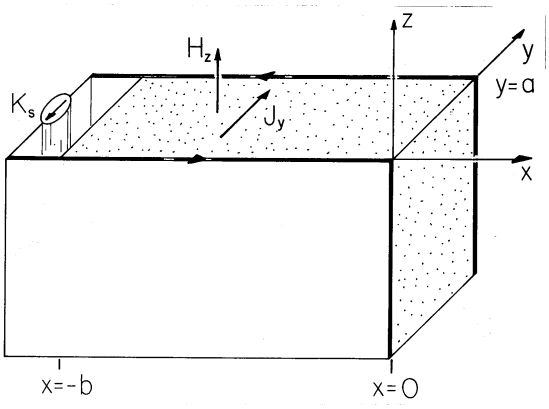

Fig. 10.6.1 A block of uniformly conducting material having length b and thickness a is sandwiched between perfectly conducting electrodes that are driven along their edges at $x = -b$ by a distributed current source. Current density and field intensity in the block are, respectively, y and z directed, each depending on (x, t).

that shown in Fig. 10.5.1, where the current density is transverse to a magnetic field intensity that has only one component, H_z.

If this field and the associated current density are indeed independent of y, then it follows from (10.5.10) and (10.5.11) that H_z satisfies the one-dimensional diffusion equation

$$\frac{1}{\mu\sigma}\frac{\partial^2 H_z}{\partial x^2} = \frac{\partial H_z}{\partial t} \tag{1}$$

and the only component of the current density is related to H_z by Ampère's law

$$\mathbf{J} = -\mathbf{i_y}\frac{\partial H_z}{\partial x} \tag{2}$$

Note that this one-dimensional model correctly requires that the current density, and hence the electric field intensity, be normal to the perfectly conducting electrodes at $y = 0$ and $y = a$.

The distributed current source, perfectly conducting sheets and conducting block form a closed path for currents that circulate in $x-y$ planes. These extend to infinity in the $+$ and $-z$ directions in the manner of an infinite one-turn solenoid. The field outside the outermost of these current paths is therefore taken as being zero. Ampère's continuity condition then requires that at the surface $x = -b$, where the distributed current source is located, the enclosed magnetic field intensity be equal to the imposed surface current density K_s. In the plane $x = 0$, the situation is similar except that there is no surface current density, and so the magnetic field intensity must be zero. Thus, consistent with solving a differential equation that is second order in x, are the two boundary conditions

$$H_z(-b, t) = K_s(t), \qquad H_z(0, t) = 0 \tag{3}$$

The equation is first order in its time dependence, suggesting that to complete the specification of the transient solution, the initial value of H_z must also be given.

$$H_z(x, 0) = H_i(x) \tag{4}$$

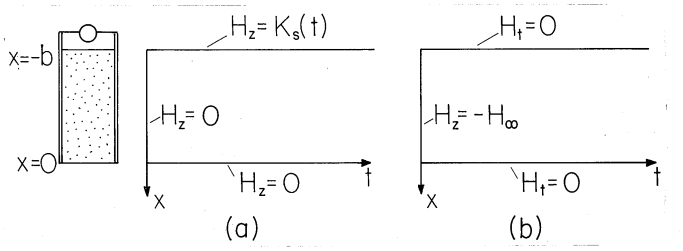

Fig. 10.6.2 Boundary and initial conditions for one-dimensional magnetic diffusion pictured in the $x - t$ plane. (a) The total fields at the ends of the block are constrained to be equal to the driving surface current density and to zero, respectively, while there is one initial condition when $t = 0$. (b) The transient part of the solution is zero at the boundaries and satisfies the initial condition that makes the total solution assume the current value when $t = 0$.

It is helpful to picture the boundary and initial conditions needed to uniquely specify solutions to (2) in the $x - t$ plane, as shown in Fig. 10.6.2a. Here the conducting block can be pictured as extending from $x = 0$ to $x = -b$, with the field between a function of x that evolves in the t "direction." Presumably, the distribution of H_z in the $x-t$ space is predicted by (1) with the boundary conditions of (3) at $x = 0$ and $x = -b$ and the initial condition of (4) when $t = 0$.

Is the solution for $H_z(t)$ uniquely specified by (1), the boundary conditions of (3), and the initial condition of (4)? A proof that it is can be made following a line of reasoning suggested by the EQS uniqueness arguments of Sec. 7.8.

Suppose that the drive is a step function of time, so that the final state is one of uniform steady conduction. Then, the linearity of (1) makes it possible to think of the total field as being the superposition of this steady field and a transient part.

$$H_z = H_\infty(x) + H_t(x,t) \tag{5}$$

The steady solution, which presumably prevails as $t \to \infty$, satisfies (1) with the time derivative set equal to zero,

$$\frac{\partial^2 H_\infty}{\partial x^2} = 0 \tag{6}$$

while the transient part satisfies the complete equation.

$$\frac{1}{\mu\sigma}\frac{\partial^2 H_t}{\partial x^2} = \frac{\partial H_t}{\partial t} \tag{7}$$

Because the steady solution satisfies the boundary conditions for all time $t > 0$, the boundary conditions satisfied by the transient part are homogeneous.

$$H_t(-b,t) = 0; \qquad H_t(0,t) = 0 \tag{8}$$

However, the steady solution does not satisfy the initial condition. The transient solution is therefore adjusted so that the total solution does.

$$H_t(x,0) = H_i(x) - H_\infty(x) \tag{9}$$

The conditions satisfied by the transient part of the solution on the boundaries in the $x-t$ space are pictured in Fig. 10.6.2b.

Product Solutions to the One-Dimensional Diffusion Equation. The approach now used to find the H_t that satisfies (7) and the conditions of (8) and (9) is familiar from finding Cartesian coordinate product solutions to Laplace's equation in two dimensions in Sec. 5.4. Here the second "dimension" is t and we consider solutions that take the form $H_t = X(x)T(t)$. Substitution into (7) and division by XT gives

$$\frac{1}{X}\frac{d^2X}{dx^2} - \frac{\mu\sigma}{T}\frac{dT}{dt} = 0 \tag{10}$$

With the first term taken as $-k^2$ and the second as k^2, it follows that

$$\frac{1}{X}\frac{d^2X}{dx^2} = -k^2 \Rightarrow \frac{d^2X}{dx^2} + k^2X = 0 \tag{11}$$

and

$$-\frac{\mu\sigma}{T}\frac{dT}{dt} = k^2 \Rightarrow \frac{dT}{dt} + \frac{k^2}{\mu\sigma}T = 0 \tag{12}$$

Given the boundary conditions of (8), the appropriate solution to (11) is

$$X = \sin kx; \qquad k = \frac{n\pi}{b} \tag{13}$$

where n can be any integer. Associated with each of these modes is a time dependence given by (12) as a decaying exponential with the time constant

$$\tau_n = \frac{\mu\sigma b^2}{(n\pi)^2} \tag{14}$$

Thus, we are led to a transient part of the solution that is itself a superposition of modes, each satisfying the boundary conditions.

$$H_t = \sum_{n=1}^{\infty} C_n \sin\left(\frac{n\pi}{b}x\right)e^{-t/\tau_n} \tag{15}$$

When $t = 0$, the modes take the form of a Fourier series. Thus, the coefficients C_n can be used to satisfy the initial condition, (9).

In the following example, the coefficients are evaluated for specific initial conditions. However, because the "short time" and "long time" field and current distributions are known at the outset, much of the dynamics can be anticipated at the outset. For times that are very short compared to the magnetic diffusion time $\mu\sigma b^2$, the conducting block must act as a perfect conductor. In this short time limit, we know from Chap. 8 that the current from the distributed source is confined to the surface at $x = -b$. Thus, for early times, the distribution represented by the series of (15) tends to be an impulse function of x. After many magnetic diffusion

times, the current reaches a steady state and achieves a distribution that would be predicted in the first half of Chap. 7. The following example fills in the evolution from the field of a perfectly conducting system to that for steady conduction.

Example 10.6.1. Response to a Step in Current

When $t = 0$, suppose that there are no currents or associated fields. Then the current source suddenly becomes the constant K_p. The solution to (6) that is zero at $x = 0$ and is K_p at $x = -b$ is

$$H_\infty = -K_p \frac{x}{b} \tag{16}$$

This is the field associated with a constant current density K_p/b that is uniformly distributed over the cross-section of the block.

Because there is no initial magnetic field, it follows from (9) that the initial transient part of the field must cancel the steady part.

$$H_t(x,0) = K_p \frac{x}{b} \tag{17}$$

This must be the distribution of H_t given by (15) when $t = 0$.

$$K_p \frac{x}{b} = \sum_{n=1}^{\infty} C_n \sin\left(\frac{n\pi}{b}x\right) \tag{18}$$

Following the procedure familiar from Sec. 5.5, the coefficients C_n are now evaluated by multiplying both sides of this expression by $\sin(m\pi/b)$, multiplying by dx, and integrating from $x = -b$ to $x = 0$.

$$\int_{-b}^{0} K_p \frac{x}{b} \sin\left(\frac{m\pi}{b}x\right)dx = \sum_{n=1}^{\infty} C_n \int_{-b}^{0} \sin\left(\frac{n\pi}{b}x\right)\sin\left(\frac{m\pi}{b}x\right)dx \tag{19}$$

From the series on the right, only the term $m = n$ is not zero. Carrying out the integration on the left[3] then gives an expression that can be solved for C_m. Replacing $m \to n$ then gives

$$C_n = -2K_p \frac{(-1)^n}{n\pi} \tag{20}$$

Finally, (16) and (15) [the latter evaluated using (20)] are superimposed as required by (5) to give the desired description of how the field evolves as a function of space and time.

$$H_z = -K_p \frac{x}{b} - \sum_{n=1}^{\infty} 2K_p \frac{(-1)^n}{n\pi} \sin\left(\frac{n\pi x}{b}\right) e^{-t/\tau_n} \tag{21}$$

The distribution of current density follows from this expression substituted into Ampère's law, (2).

$$J_y = \frac{K_p}{b} + \sum_{n=1}^{\infty} 2K_p \frac{(-1)^n}{b} \cos\left(\frac{n\pi x}{b}\right) e^{-t/\tau_n} \tag{22}$$

[3] $\int \sin(u)u\,du = \sin(u) - u\cos(u)$

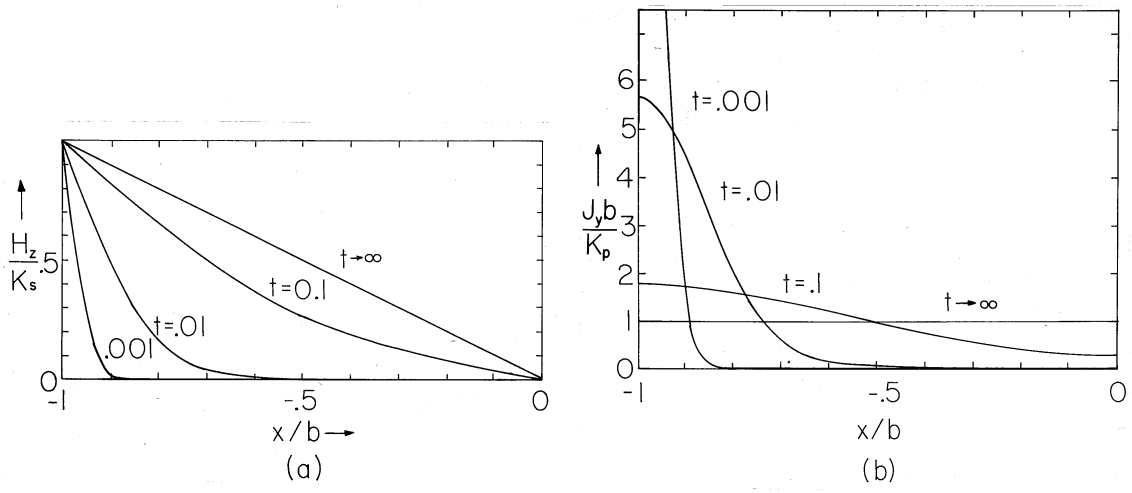

Fig. 10.6.3 (a) Distribution of H_z in the conducting block of Fig. 10.6.1 in response to applying a step in current with no initial field. In terms of time normalized to the magnetic diffusion time based on the length b, the field diffuses into the block, finally assuming the linear distribution expected for steady conduction. (b) Distribution of J_y with normalized time as a parameter. The initial distribution is an impulse (a surface current density) at $x = -b$, while the final distribution is uniform.

These expressions are pictured in Fig. 10.6.3. Note that the higher the order of a term, the more rapid its exponential decay with time. As a result, the most terms in the series are needed when $t = 0^+$. These are needed to make the initial magnetic field intensity zero and the initial current density an impulse at $x = -b$. Because the lowest mode in the transient part of either H_z or J_y has the longest time constant, the long-time response is dominated by the steady response and the first term in the series. Of course, with the decay of the transient part, the field approaches a linear x dependence while the current density assumes the uniform distribution expected for a steady current.

10.7 SKIN EFFECT

If the surface current source driving the conducting block of Fig. 10.6.1 is a sinusoidal function of time

$$K_s(t) = Re\hat{K}_s e^{j\omega t} \tag{1}$$

the current density tends to circulate through the block in the neighborhood of the surface adjacent to the source. This tendency for the sinusoidal steady state current to return to the source through the thin zone or skin region nearest to the source gives another view of magnetic diffusion.

To illustrate skin effect in specific terms we return to the one-dimensional diffusion configuration of Sec. 10.6, Fig. 10.6.1. Once again, the distributions of H_z

and J_y are governed by the one-dimensional diffusion equation and Ampère's law, (10.6.1) and (10.6.2).

The diffusion equation is linear and has coefficients that are independent of time. We can expect a sinusoidal steady state response having the same frequency as the drive, (1). The solution to the diffusion equation is therefore taken as having a product form, but with the time dependence stipulated at the outset.

$$H_z = Re\hat{H}_z(x)e^{j\omega t} \tag{2}$$

At a given location x, the coefficient of the exponential is a complex number specifying the magnitude and phase of the field.

Substitution of (2) into the diffusion equation, (10.6.1), shows that the complex amplitude has an x dependence governed by

$$\frac{d^2\hat{H}_z}{dx^2} - \gamma^2\hat{H}_z = 0 \tag{3}$$

where $\gamma^2 \equiv j\omega\mu\sigma$.

Solutions to (3) are simply $\exp(\mp\gamma x)$. However, γ is complex. If we note that $\sqrt{j} = (1+j)/\sqrt{2}$, then it follows that

$$\gamma = \sqrt{j\omega\mu\sigma} = (1+j)\sqrt{\frac{\omega\mu\sigma}{2}} \tag{4}$$

In terms of the *skin depth* δ, defined by

$$\delta \equiv \sqrt{\frac{2}{\omega\mu\sigma}} \tag{5}$$

One can also write (4) as

$$\gamma = \frac{(1+j)}{\delta} \tag{6}$$

With C_+ and C_- arbitrary coefficients, solutions to (3) are therefore

$$\hat{H}_z = C_+e^{-(1+j)\frac{x}{\delta}} + C_-e^{(1+j)\frac{x}{\delta}} \tag{7}$$

Before considering a detailed example where these coefficients are evaluated using the boundary conditions, consider the $x-t$ dependence of the field represented by the first solution in (7). Substitution into (2) gives

$$H_z = Re\left[C_1e^{-\frac{x}{\delta}}e^{j(\omega t-\frac{x}{\delta})}\right] \tag{8}$$

making it clear that the field magnitude is an exponentially decaying function of x. Within the envelope with the decay length δ shown in Fig. 10.7.1, the field propagates in the x direction. That is, points of constant phase on the field distribution have $\omega t - x/\delta =$ constant and hence move in the x direction with the velocity $\omega\delta$.

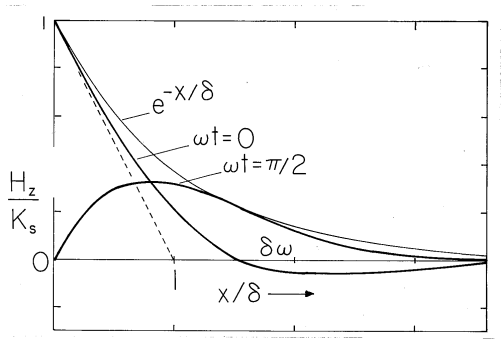

Fig. 10.7.1 Magnetic diffusion wave in the sinusoidal steady state, showing envelope with decay length δ and instantaneous field at two different times. The point of zero phase propagates with the velocity $\omega\delta$.

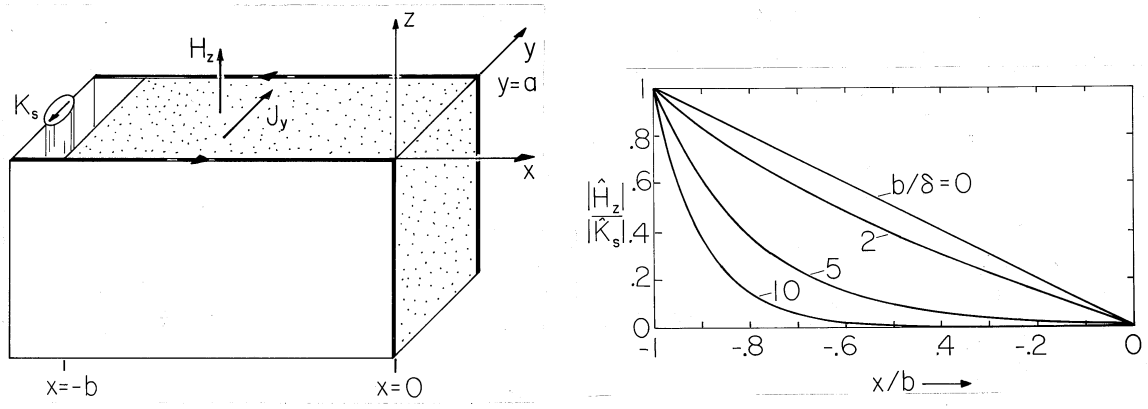

Fig. 10.7.2 (a) One-dimensional magnetic diffusion in the sinusoidal steady state in the same configuration as considered in Sec. 10.6. (b) Distribution of the magnitude of H_z in the conducting block of (a) as a function of the skin depth. Decreasing the skin depth is equivalent to raising the frequency.

Although the phase propagation signifies that at a given instant, the field (and current density) are positive in one region while negative in another, the propagation is difficult to discern because the decay is very rapid.

The second solution in (7) represents a similar diffusion wave, but decaying and propagating in the $-x$ rather than the $+x$ direction. The following illustrates how the two diffusion waves combine to satisfy boundary conditions.

Example 10.7.1. Diffusion into a Conductor of Finite Thickness

We consider once again the field distribution in a conducting material sandwiched between perfectly conducting plates, as shown in either Fig. 10.7.2 or Fig. 10.6.1. The surface current density of the drive is given by (1) and it is assumed that any transient reflecting the initial conditions has died out. How does the frequency dependence of the field distribution in the conducting block reflect the magnetic diffusion process?

Boundary conditions on H_z are the same as in Sec. 10.6, $H_z(-b,t) = K_s(t)$ and $H_z(0,t) = 0$. These are satisfied by adjusting the complex amplitude so that

$$\hat{H}_z(-b) = \hat{K}_s; \qquad \hat{H}_z(0) = 0 \tag{9}$$

It follows from (7) that the second of these is satisfied if $C_+ = -C_-$. The first condition then serves to evaluate C_+ and hence C_-, so that

$$\hat{H}_z = \hat{K}_s \frac{\left(e^{-(1+j)\frac{x}{\delta}} - e^{(1+j)\frac{x}{\delta}}\right)}{\left(e^{(1+j)\frac{b}{\delta}} - e^{-(1+j)\frac{b}{\delta}}\right)} \tag{10}$$

This expression represents the superposition of fields propagating and decaying in the $\pm x$ directions, respectively. Evaluated at a given location x, it is a complex number. In accordance with (2), H_z is the real part of this number multiplied by $\exp(j\omega t)$. The magnitude of H_z is the magnitude of (10), and is shown with the skin depth as a parameter by Fig. 10.7.2.

Consider the field distribution in two limits. First, suppose that the skin depth is very large compared to the thickness b of the conducting block. This might be the limit in which the frequency is made very low compared to the reciprocal magnetic diffusion time based on the conductor thickness.

$$\delta \gg b \Rightarrow \frac{2}{\omega\mu\sigma} \gg b^2 \Rightarrow \frac{2}{\mu\sigma b^2} \gg \omega \tag{11}$$

In this limit, the arguments of the exponentials in (10) are small. Using the approximation $\exp(u) \approx 1 + u$, (10) becomes

$$\hat{H}_z \to \hat{K}_s \frac{\left[1 - (1+j)\frac{x}{\delta}\right] - \left[1 + (1+j)\frac{x}{\delta}\right]}{\left[1 + (1+j)\frac{b}{\delta}\right] - \left[1 - (1+j)\frac{b}{\delta}\right]} = -\hat{K}_s \frac{x}{b} \tag{12}$$

Substitution of this complex amplitude into (2) gives the space-time dependence.

$$H_z \to \frac{-x}{b} Re\hat{K}_s e^{j\omega t} \tag{13}$$

The field has the linear distribution expected if the current density is uniformly distributed over the length of the conductor. In this large skin depth limit, the field and current density spatial distributions are essentially the same as if the current source were time independent.

In the opposite extreme, the skin depth is short compared to the conductor length. Perhaps this is accomplished by making the frequency very high compared to the reciprocal magnetic diffusion time based on the conductor length.

$$\delta \ll b \Rightarrow \frac{2}{\mu\sigma b^2} \ll \omega \tag{14}$$

Then, the first term in the denominator of (10) is large compared with the second. Division of the numerator by this first term gives

$$\hat{H}_z \to \hat{K}_s \left[e^{-(1+j)\frac{x+b}{\delta}} - e^{(1+j)\frac{x-b}{\delta}}\right] \approx \hat{K}_s e^{-(1+j)\left(\frac{x+b}{\delta}\right)} \tag{15}$$

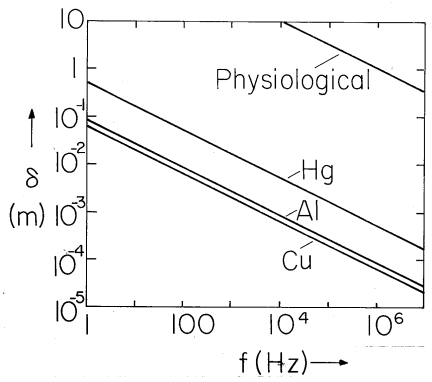

Fig. 10.7.3 Skin depth as a function of frequency.

In justifying the second of these expressions, remember that x is negative throughout the region of interest. Substitution of (15) into (2) shows that in this short skin depth limit

$$H_z = Re\left\{\hat{K}_s e^{-\left(\frac{(x+b)}{\delta}\right)} e^{j\left[\omega t - \frac{(x+b)}{\delta}\right]}\right\} \tag{16}$$

With the origin shifted from $x = 0$ to $x = -b$, this field has the $x - t$ dependence of the diffusion wave represented by (8). So it is that in the short skin depth limit, the distribution of the field magnitude shown in Fig. 10.7.2 has the exponential decay typical of skin effect.

The skin depth, (5), is inversely proportional to the square root of $\omega\mu\sigma$. Thus, an order of magnitude variation in frequency or in conductivity only changes δ by about a factor of about 3. Even so, skin depths found under practical conditions are widely varying because these parameters have enormous ranges. In good conductors, such as copper or aluminum, Fig. 10.7.3 illustrates how δ varies from about 1 cm at 60 Hz to less than 0.1 mm at l MHz. Of interest in determining magnetically induced currents in flesh is the curve for skin depth in materials having the "physiological" conductivity of about 0.2 S/m (Demonstration 7.9.1).

If the frequency is high enough so that the skin depth is small compared with the dimensions of interest, then the fields external to the conductor are essentially determined using the perfect conductivity model introduced in Sec. 8.4. In Demonstration 8.6.1, the fields around a conductor above a ground plane line were derived and the associated surface current densities deduced. If these currents are in the sinusoidal steady state, we can now picture them as actually extending into the conductors a distance that is on the order of δ.

Although skin effect determines the paths of current flow at radio frequencies, as the following demonstrates, it can be important even at 60 Hz.

Demonstration 10.7.1. Skin Effect

The core of magnetizable material shown in Fig. 10.7.4 passes through a slit cut from an aluminum block and through a winding that is driven at a frequency in the range of 60–240 Hz. The winding and the block of aluminum, respectively, comprise

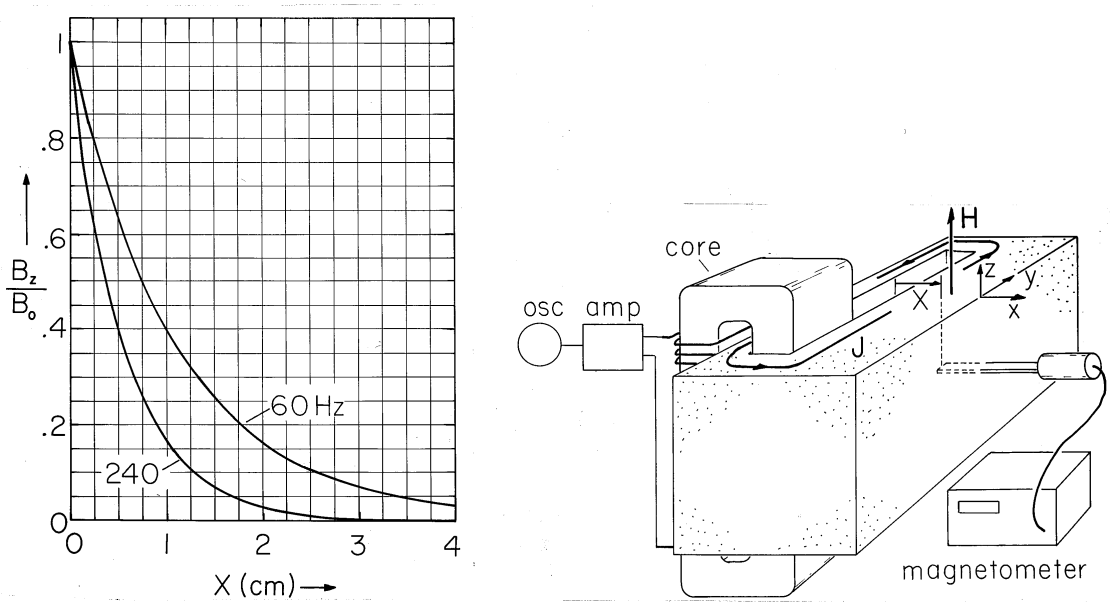

Fig. 10.7.4 Demonstration of skin effect. Currents induced in the conducting block tend to follow paths of minimum reactance nearest to the slot. Thus, because the aluminum block is thick compared to the skin depth, the field intensity observed decreases exponentially with distance X. In the experiment, the block is $10 \times 10 \times 26$ cm with thickness of 6 cm between the right face of the slot and the right side of the block. In aluminum at 60 Hz, $\delta = 1.1$ cm, while at 240 Hz δ is half of that. To avoid distortion of the field, the yoke is placed at one end of the slot.

the primary and secondary of a transformer. In effect, the secondary is composed of one turn that is shorted on itself.

The thickness b of the aluminum block is somewhat larger than a skin depth at 60 Hz. Therefore, currents circulating through the block around the leg of the magnetic circuit tend to follow the paths of least reactance closest to the slit. By making the length of the block and slit in the y direction large compared to b, we expect to see distributions of current density and associated magnetic field intensity at locations in the block well removed from the ends that have the x dependence found in Example 10.7.1.

In the limit where δ is small compared to b, the magnitude of the expected magnetic flux density B_z (normalized to its value where $X = 0$) has the exponential decay with distance x of the inset to Fig. 10.7.4. The curves shown are for aluminum at frequencies of 60 Hz and 240 Hz. According to (5), increasing the frequency by a factor of 4 should decrease the skin depth by a factor of 2. Provision is made for measuring this field by having a small slit milled in the block with a large enough width to permit the insertion of a magnetometer probe oriented to measure the magnetic flux density in the z direction.

As we have seen in this and previous sections, currents induced in a conductor tend to exclude the magnetic field from some region. Conductors are commonly used as shields that isolate a region from its surroundings. Typically, the conductor is made thick compared to the skin depth based on the fields to be shielded out.

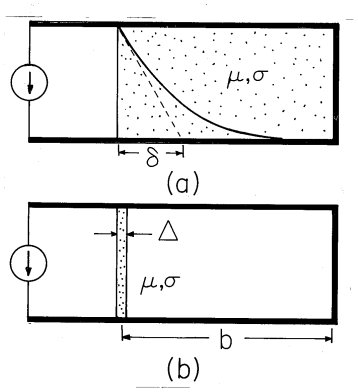

Fig. 10.7.5 Perfectly conducting ⊃-shaped conductors are driven by a distributed current source at the left. The magnetic field is shielded out of the region to the right enclosed by the perfect conductors by: (a) a block of conductor that fills the region and has a thickness b that is large compared to a skin depth; and (b) a sheet conductor having a thickness Δ that is less than the skin depth.

However, our studies of currents induced in thin conducting shells in Secs. 10.3 and 10.4 make it clear that this can be too strict a requirement for good shielding. The thin-sheet model can now be seen to be valid if the skin depth δ is *large* compared to the thickness Δ of the sheet. Yet, we found that for a cylindrical shell of radius R, provided that $\omega\mu\sigma\Delta R \gg 1$, a sinusoidally varying applied field would be shielded from the interior of the shell. Apparently, under certain circumstances, even a conductor that is thin compared to a skin depth can be a good shield.

To understand this seeming contradiction, consider the one-dimensional configurations shown in Fig. 10.7.5. In the first of the two, plane parallel perfectly conducting electrodes again sandwich a block of conductor in a system that is very long in a direction perpendicular to the paper. However, now the plates are shorted by a perfect conductor at the right. Thus, at very low frequencies, all of the current from the source circulates through the perfectly conducting plates, bypassing the block. As a result, the field throughout the conductor is uniform. As the frequency is raised, the electric field generated by the time-varying magnetic flux drives a current through the block much as in Example 10.7.1, with the current in the block tending to circulate through paths of least reactance near the left edge of the block. For simplicity, suppose that the skin depth δ is shorter than the length of the block b, so that the decay of current density and field into the block is essentially the exponential sketched in Fig. 10.7.5a. With the frequency high enough to make the skin depth short compared to b, the field tends to be shielded from points within the block.

In the configuration of Fig. 10.7.5b, the block is replaced by a sheet having the same σ and μ but a thickness Δ that is less than a skin depth δ. Is it possible that this thin sheet could suppress the field in the region to the right as well as the thick conductor?

The answer to this question depends on the location of the observer and the extent b of the region with which he or she is associated. In the conducting block, shielding is poor in the neighborhood of the left edge but rapidly improves at

distances into the interior that are of the order of δ or more. By contrast, the sheet conductor can be represented as a current divider. The surface current, K_s, of the source is tapped off by the sheet of conductivity per unit width $G = \sigma\Delta/h$ (where h is the height of the structure) connected to the inductance (assigned to unit width) $L = \mu bh$ of the single-turn inductor. The current through the single-turn inductor is

$$K_s \frac{1/j\omega L}{\left(G + \frac{1}{j\omega L}\right)} = \frac{K_s}{1 + j\omega LG} \tag{17}$$

This current, and the associated field, is shielded out effectively when $|\omega LG| = \omega\mu\sigma b\Delta \gg 1$. With the sheet, the shielding strategy is to make equal use of all of the volume to the right for generating an electric field in the sheet conductor. The efficiency of the shielding is improved by making $\omega\mu\sigma\Delta b$ large: The interior field is made small by making the shielded volume large.

10.8 SUMMARY

Before tackling the concepts in this chapter, we had studied MQS fields in two limiting situations:

- In the first, currents in Ohmic conductors were essentially stationary, with distributions governed by the steady conduction laws investigated in Secs. 7.2–7.6. The associated magnetic fields were then found by using these current distributions as sources. In the absence of magnetizable material, the Biot-Savart law of Sec. 8.2 could be used for this purpose. With or without magnetizable material, the boundary value approaches of Secs. 8.5 and 9.6 were applicable.
- In the second extreme, where fields were so rapidly varying that conductors were "perfect," the effect on the magnetic field of currents induced in accordance with the laws of Faraday, Ampère, and Ohm was to nullify the magnetic flux density normal to conducting surfaces. The boundary value approach used to find self-consistent fields and surface currents in this limit was the subject of Secs. 8.4 and 8.6.

In this chapter, the interplay of the laws of Faraday, Ohm, and Ampère has again been used to find self-consistent MQS fields and currents. However, in this chapter, the conductivity has been finite. This has made it possible to explore the dynamics of fields with source currents that were neither distributed throughout the volumes of conductors in accordance with the laws of steady conduction nor confined to the surfaces of perfect conductors.

In dealing with perfect conductors in Chaps. 8 and 9, the all-important role of $\mathbf{E}$ could be placed in the background. Left for a study of this chapter was the electric field induced by a time-varying magnetic induction. So, we began in Sec. 10.1 by picturing the electric field in systems of perfect conductors. The approach was familiar from solving EQS (Chap. 5) and MQS (Chap. 8) boundary value problems involving Poisson's equation. The electric field intensity was represented by the superposition of a particular part having a curl that balanced $-\partial\mathbf{B}/\partial t$ at

each point in the volume, and an irrotational part that served to make the total field tangential to the surfaces of the perfect conductors.

Having developed some insight into the rotational electric fields induced by magnetic induction, we then undertook case studies aimed at forming an appreciation for spatial and temporal distributions of currents and fields in finite conductors. By considering the effects of finite conductivity, we could answer questions left over from the previous two chapters.

- Under what conditions are distributions of current and field quasistationary in the sense of being essentially snapshots of a sequence of static fields?
- Under what conditions do they consist of surface currents and fields having negligible normal components at the surfaces of conductors?

We now know that the answer comes in terms of characteristic magnetic diffusion (or relaxation) times τ that depend on the electrical conductivity, the permeability, and the product of lengths.

$$\tau = \mu\sigma\Delta b \tag{1}$$

The lengths in this expression make it clear that the size and topology of the conductors plays an important role. This has been illustrated by the thin-sheet models of Secs. 10.3 and 10.4 and one-dimensional magnetic diffusion into the bulk of conductors in Secs. 10.6 and 10.7. In each of these classes of configurations, the role played by τ has been illustrated by the step response and by the sinusoidal steady state response. For the former, the answer to the question, "When is a conductor perfect?" was literal. The conductor tended to be perfect for times that were short compared to a properly defined τ. For the latter, the answer came in the form of a condition on the frequency. If $\omega\tau \gg 1$, the conductor tended to be perfect.

In the sinusoidal state, a magnetic field impressed at the surface of a conductor penetrates a distance δ into the conductor that is the skin depth and is given by setting $\omega\tau = \omega\mu\sigma\delta^2 = 2$ and solving for δ.

$$\delta = \sqrt{\frac{2}{\omega\mu\sigma}} \tag{2}$$

It is true that conductors will act as perfect conductors if this skin depth is much shorter than all other dimensions of interest. However, the thin sheet model of Sec. 10.4 teaches the important lesson that the skin depth may be larger than the conductor thickness and yet the conductor can still act to shield out the normal flux density. Indeed, in Sec. 10.4 it was assumed that the current was uniform over the conductor cross-section and hence that the skin depth was large, not small, compared to the conductor thickness. Demonstration 8.6.1, where current passes through a cylindrical conductor at a distance l above a conducting ground plane, is an example. It would be found in that demonstration that if l is large compared to the conductor thickness, the surface current in the ground plane would distribute itself in accordance with the perfectly conducting model even if the frequency is so low that the skin depth is somewhat larger than the thickness of the ground plane. If Δ is the ground plane thickness, we would expect the normal flux density to be small so long as $\omega\tau_m = \omega\mu\sigma\Delta l \gg 1$. Typical of such situations is that the electrical dissipation due to conduction is confined to thin conductors and the magnetic

energy storage occupies relatively larger regions that are free of dissipation. Energy storage and power dissipation are subjects taken up in the next chapter.

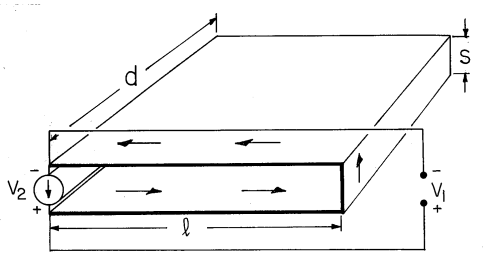

Fig. P10.0.2

PROBLEMS

10.1 Introduction

10.1.1* In Demonstration 10.0.1, the circuit formed by the pair of resistors is replaced by the one shown in Fig. 10.0.1, composed of four resistors of equal resistance R. The voltmeter might be the oscilloscope shown in Fig. 10.0.1. The "grounded" node at (4) is connected to the negative terminal of the voltmeter.

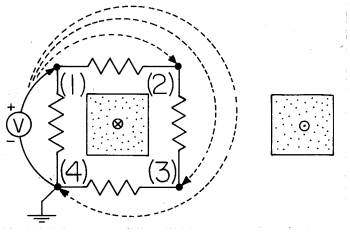

Fig. P10.0.1

(a) Show that the voltage measured with the positive lead connected at (1), so that the voltmeter is across one of the resistors, is $v = (d\Phi_\lambda/dt)/4$.

(b) Show that if the positive voltmeter lead is connected to (2), then to (3), and finally to (4) (so that the lead is wrapped around the core once and connected to the same grounded node as the negative voltmeter lead), the voltages are, respectively, twice, three times, and four times this value. Show that this last result is as would be expected for a transformer with a one-turn secondary.

10.1.2 Plane parallel perfectly conducting plates are shorted to form the one-turn inductor shown in Fig. 10.0.2. The current source is distributed so that it supplies i amps over the width d.

(a) Given that d and l are much greater than the spacing s, determine the voltage measured across the terminals of the current source by the voltmeter v_2.

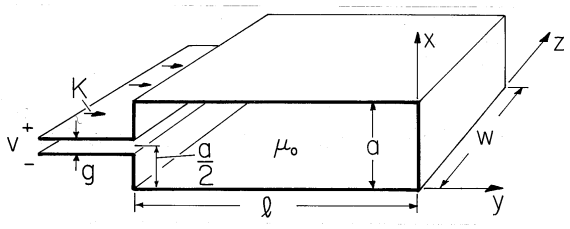

Fig. P10.1.2

(b) What is the voltage measured by the voltmeter v_1 connected as shown in the figure across these same terminals?

10.2 Magnetoquasistatic Electric Fields in Systems of Perfect Conductors

10.2.1* In Prob. 8.4.1, the magnetic field of a dipole surrounded by a perfectly conducting spherical shell is found. Show that

$$\mathbf{E} = \mathbf{i}_\phi \frac{\mu_o a^2}{4R^2} \frac{dI}{dt} \left[\frac{r}{R} - (R/r)^2 \right] \sin\theta \qquad (a)$$

in the region between the dipole and the shell.

10.2.2 The one-turn inductor of Fig. P10.1.2 is driven at the left by a current source that evenly distributes the surface current density $K(t)$ over the width w. The dimensions are such that $g \ll a \ll w$.

(a) In terms of $K(t)$, what is $\mathbf{H}$ between the plates?
(b) Determine a particular solution having the form $\mathbf{E}_p = \mathbf{i}_\mathbf{x} E_{xp}(y,t)$, and find $\mathbf{E}$.

10.2.3 The one-turn solenoid shown in cross-section in Fig. P10.1.3 consists of perfectly conducting sheets in the planes $\phi = 0$, $\phi = \alpha$, and $r = a$. The latter is broken at the middle and driven by a current source of $K(t)$ amps/unit length in the z direction. The current circulates around the perfectly conducting path provided by the sheets, as shown in the figure. Assume that the angle $\alpha \gg \delta$ and that the system is long enough in the z direction to justify taking the fields as two dimensional.

(a) In terms of $K(t)$, what is $\mathbf{H}$ in the pie-shaped region?
(b) What is $\mathbf{E}$ in this region?

10.2.4* By constrast with previous examples and problems in this section, consider here the induction of currents in materials that have relatively *low* conductivity. An example would be the induction heating of silicon in the manufacture of semiconductor devices. The material in which the currents are to be induced takes the form of a long circular cylinder of radius b.

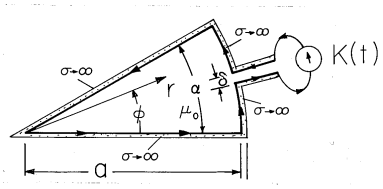

Fig. P10.1.3

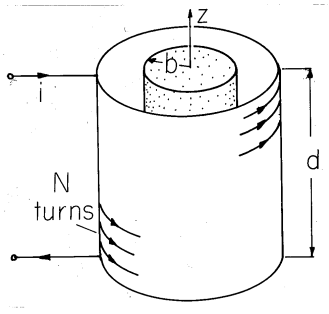

Fig. P10.1.4

A long solenoid surrounding this material has N turns, a length d that is much greater than its radius, and a driving current $i(t)$, as shown in Fig. P10.1.4.

Because the material to be heated has a small conductivity, the induced currents are small and contribute a magnetic field that is small compared to that imposed. Thus, the approach to determining the distribution of current induced in the semiconductor is 1) to first find $\mathbf{H}$, ignoring the effect of the induced current. This amounts to solving Ampère's law and the flux continuity law with the current density that of the excitation coil. Then, 2) with $\mathbf{B}$ known, the electric field in the semiconductor is determined using Faraday's law and the MQS form of the conservation of charge law, $\nabla \cdot (\sigma \mathbf{E}) = 0$. The approach to finding the fields can then be similar to that illustrated in this section.

(a) Show that in the semiconductor and in the annulus, $\mathbf{B} \approx (\mu_o N i/d)\mathbf{i_z}$.
(b) Use the symmetry about the z axis to show that in the semiconductor, where there is no radial component of $\mathbf{J}$ and hence of $\mathbf{E}$ at $r = b$, $\mathbf{E} = -(\mu_o N r/2d)(di/dt)\mathbf{i}_\phi$.
(c) To investigate the conditions under which this approximation is useful, suppose that the excitation is sinusoidal, with angular frequency ω. Approximate the magnetic field intensity $H_{induced}$ associated with the induced current. Show that for the approximation to be good, $H_{induced}/H_{imposed} = \omega \mu_o \sigma b^2/4 \ll 1$.

10.2.5 The configuration for this problem is the same as for Prob. 10.1.4 except that the slightly conducting material is now a cylinder having a rectangular cross-section, as shown in Fig. P10.1.5. The imposed field is therefore the same as before.

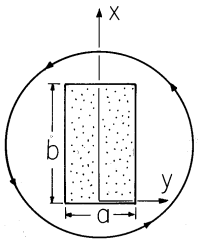

Fig. P10.1.5

(a) In terms of the coordinates shown, find a particular solution for $\mathbf{E}$ that takes the form $\mathbf{E} = \mathbf{i_y} E_{yp}(x,t)$ and satisfies the boundary conditions at $x = 0$ and $x = b$.
(b) Determine $\mathbf{E}$ inside the material of rectangular cross-section.
(c) Sketch the particular, homogeneous, and total electric fields, making clear how the first two add up to satisfy the boundary conditions. (Do not take the time to evaluate your analytical formula but rather use your knowledge of the nature of the solutions and the boundary conditions that they must satisfy.)

10.3 Nature of Fields Induced in Finite Conductors

10.3.1* The "Boomer" might be modeled as a transformer, with the disk as the one-turn secondary terminated in its own resistance. We have found here that if $\omega\tau_m \gg 1$, then the flux linked by the secondary is small. In Example 9.7.4, it was shown that operation of a transformer in its "ideal" mode also implies that the flux linked by the secondary be small. There it was found that to achieve this condition, the time constant L_{22}/R of the secondary must be long compared to times of interest. Approximate the inductance and resistance of the disk in Fig. 10.2.3 and show that L_{22}/R is indeed roughly the same as the time given by (10.2.17).

10.3.2 It is proposed that the healing of bone fractures can be promoted by the passage of current through the bone normal to the fracture. Using magnetic induction, a transient current can be induced without physical contact with the patient. Suppose a nonunion of the radius (a nonhealing fracture in the long bone of the forearm, as shown in Fig. P10.2.2) is to be treated. How would you arrange a driving coil so as to induce a longitudinal current along the bone axis through the fracture?

10.3.3* Suppose that a driving coil like that shown in Fig. 10.2.2 is used to produce a magnetic flux through a conductor having the shape of the circular cylindrical shell shown in Fig. 10.3.2. The shell has a thickness Δ and radius a. Following steps parallel to those represented by (10.2.13)–(10.2.16), show that H_{ind}/H_1 is *roughly* $\omega\tau_m$, where τ_m is given by (10.3.10). (Assume that the applied field is essentially uniform over the dimensions of the shell.)

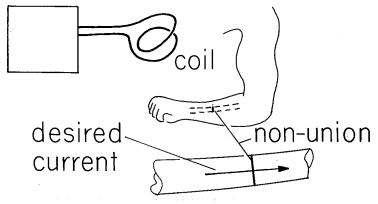

Fig. P10.2.2

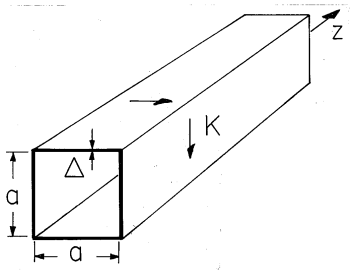

Fig. P10.3.1

10.4 Diffusion of Axial Magnetic Fields through Thin Conductors

10.4.1* A metal conductor having thickness Δ and conductivity σ is formed into a cylinder having a square cross-section, as shown in Fig. P10.3.1. It is very long compared to its cross-sectional dimensions a. When $t = 0$, there is a surface current density K_o circulating uniformly around the shell. Show that the subsequent surface current density is $K(t) = K_o \exp(-t/\tau_m)$ where $\tau_m = \mu_o \sigma \Delta a/4$.

10.4.2 The conducting sheet of thickness Δ shown in cross-section by Fig. P10.3.2 forms a one-turn solenoid having length l that is large compared to the length d of two of the sides of its right-triangular cross-section. When $t = 0$, there is a circulating current density J_o uniformly distributed in the conductor.

(a) Determine the surface current density $K(t) = \Delta J(t)$ for $t > 0$.

(b) A high-impedance voltmeter is connected as shown between the lower right and upper left corners. What $v(t)$ is measured?

(c) Now lead (1) is connected following path (2). What voltage is measured?

10.4.3* A system of two concentric shells, as shown in Fig. 10.5.2 without the center shell, is driven by the external field $H_o(t)$. The outer and inner shells have thicknesses Δ and radii a and b, respectively.

(a) Show that the fields H_1 and H_2, between the shells and inside the in-

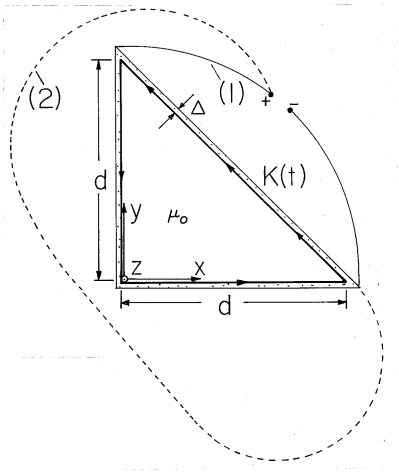

Fig. P10.3.2

ner shell, respectively, are governed by the equations ($\tau_m = \mu_o \sigma \Delta b/2$)

$$\tau_m \frac{dH_2}{dt} + H_2 - H_1 = 0 \qquad (a)$$

$$\tau_m (b/a)\frac{dH_2}{dt} + \tau_m \left(\frac{a}{b} - \frac{b}{a}\right)\frac{dH_1}{dt} + H_1 = H_o(t) \qquad (b)$$

(b) Given that $H_o = H_m \cos \omega t$, show that the sinusoidal steady state fields are $H_1 = Re\{[H_m(1+j\omega\tau_m)/D] \exp j\omega t\}$ and $H_2 = Re\{[H_m/D] \exp j\omega t\}$ where $D = [1 + j\omega\tau_m(a/b - b/a)](1 + j\omega\tau_m) + j\omega\tau_m(b/a)$.

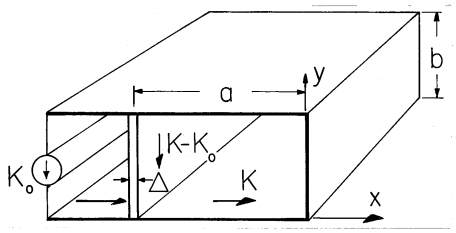

Fig. P10.3.4

10.4.4 The $\supset$-shaped perfect conductor shown in Fig. P10.3.4 is driven along its left edge by a current source having the uniformly distributed density $K_o(t)$. At $x = -a$ there is a thin sheet having the nonuniform conductivity $\sigma = \sigma_o/[1 + \alpha \cos(\pi y/b)]$. The length in the z direction is much greater than the other dimensions.

(a) Given $K_o(t)$, find a differential equation for $K(t)$.
(b) In terms of the solution $K(t)$ to this equation, determine $\mathbf{E}$ in the region $-a < x < 0,\ 0 < y < b$.

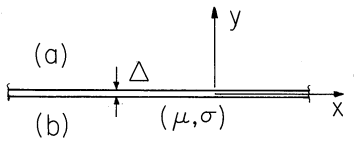

Fig. P10.4.1

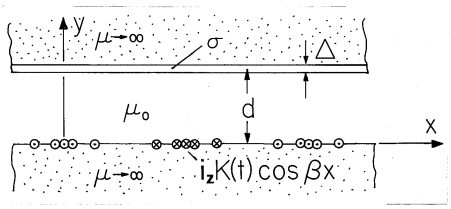

Fig. P10.4.2

10.5 Diffusion of Transverse Magnetic Fields through Thin Conductors

10.5.1* A thin planar sheet having conductivity σ and thickness Δ extends to infinity in the x and z directions, as shown in Fig. P10.4.1. Currents in the sheet are z directed and independent of z.

(a) Show that the sheet can be represented by the boundary conditions

$$B_y^a - B_y^b = 0 \qquad (a)$$

$$\frac{\partial}{\partial x}(H_x^a - H_x^b) = -\Delta\sigma\frac{\partial B_y}{\partial t} \qquad (b)$$

(b) Now consider the special case where the regions above and below are free space and extend to infinity in the $+y$ and $-y$ directions, respectively. When $t = 0$, there is a surface current density in the sheet $\mathbf{K} = \mathbf{i_z} K_o \sin\beta x$, where K_o and β are given constants. Show that for $t > 0$, $K_z = K_o \exp(-t/\tau)$ where $\tau = \mu_o\sigma\Delta/2\beta$.

10.5.2 In the two-dimensional system shown in cross-section by Fig. P10.4.2, a planar air gap of width d is bounded from above in the surface $y = d$ by a thin conducting sheet having conductivity σ and thickness Δ. This sheet is, in turn, backed by a material of infinite permeability. The region below is also infinitely permeable and at the interface $y = 0$ there is a winding used to impose the surface current density $\mathbf{K} = K(t)\cos\beta x\mathbf{i_z}$. The system extends to infinity in the $\pm x$ and $\pm z$ directions.

(a) The surface current density $K(t)$ varies so rapidly that the conducting sheet acts as a perfect conductor. What is Ψ in the air gap?

(b) The current is slowly varying so that the sheet supports little induced current. What is Ψ in the air gap?

(c) Determine $\Psi(x, y, t)$ if there is initially no magnetic field and a step, $K = K_o u_{-1}(t)$, is applied. Show that the early and long-time response matches that expected from parts (a) and (b).

10.5.3* The cross-section of a *spherical* shell having conductivity σ, radius R and thickness Δ is as shown in Fig. 8.4.5. A magnetic field that is uniform and z directed at infinity is imposed.

(a) Show that boundary conditions representing the shell are

$$B_r^a - B_r^b = 0 \qquad (a)$$

$$\frac{1}{R\sin\theta}\frac{\partial}{\partial\theta}\big[\sin\theta(H_\theta^a - H_\theta^b)\big] = -\mu_o\Delta\sigma\frac{\partial H_r}{\partial t} \qquad (b)$$

(b) Given that the driving field is $H_o(t) = Re\{\hat{H}_o\exp(j\omega t)\}$, show that the magnetic moment of a dipole at the origin that would have an effect on the external field equivalent to that of the shell is

$$\mathbf{m} = Re\{\frac{-j\omega\tau(2\pi R^3\hat{H}_o)}{1+j\omega\tau}\exp(j\omega t)\}$$

where $\tau \equiv \mu_o\sigma\Delta R/3$.

(c) Show that in the limit where $\omega\tau \to \infty$, the result is the same as found in Example 8.4.3.

10.5.4 A magnetic dipole, having moment $i(t)a$ (as defined in Example 8.3.2) oriented in the z direction is at the center of a spherical shell having radius R, thickness Δ, and conductivity σ, as shown in Fig. P10.4.4. With $i = Re\{\hat{i}\exp(j\omega t)\}$, the system is in the sinusoidal steady state.

(a) In terms of $i(t)a$, what is Ψ in the neighborhood of the origin?
(b) Given that the shell is perfectly conducting, find Ψ. Make a sketch of $\mathbf{H}$ for this limit.
(c) Now, with σ finite, determine Ψ.
(d) Take the appropriate limit of the fields found in (c) to recover the result of (b). In terms of the parameters that have been specified, under what conditions does the shell behave as though it had infinite conductivity?

10.5.5* In the system shown in cross-section in Fig. P10.4.5, a thin sheet of conductor, having thickness Δ and conductivity σ, is wrapped around a circular cylinder having infinite permeability and radius b. On the other side of an air gap at the radius $r = a$ is a winding, used to impose the surface current density $\mathbf{K} = K(t)\sin 2\phi\mathbf{i_z}$, backed by an infinitely permeable material in the region $a < r$.

(a) The current density varies so rapidly that the sheet behaves as an infinite conductor. In this limit, show that Ψ in the air gap is

$$\Psi = -\frac{aK}{2}\frac{\left[\left(\frac{r}{b}\right)^2 + \left(\frac{b}{r}\right)^2\right]}{\left[\left(\frac{a}{b}\right)^2 + \left(\frac{b}{a}\right)^2\right]}\cos 2\phi \qquad (a)$$

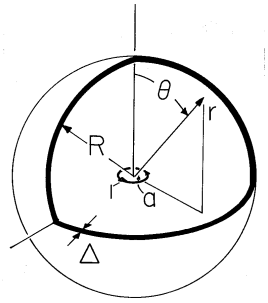

Fig. P10.4.4

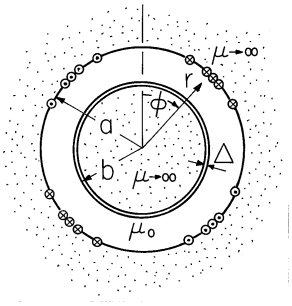

Fig. P10.4.5

(b) Now suppose that the driving current is so slowly varying that the current induced in the conducting sheet is negligible. Show that

$$\Psi = -\frac{aK}{2}\frac{\left[\left(\frac{r}{b}\right)^2 - \left(\frac{b}{r}\right)^2\right]}{\left[\left(\frac{a}{b}\right)^2 - \left(\frac{b}{a}\right)^2\right]}\cos 2\phi \qquad (b)$$

(c) Show that if the fields are zero when $t < 0$ and there is a step in current, $K(t) = K_o u_{-1}(t)$

$$\Psi = \frac{aK_o \cos 2\phi}{\left(\frac{a}{b}\right)^2 - \left(\frac{b}{a}\right)^2}\left\{\frac{\left[\left(\frac{r}{a}\right)^2 - \left(\frac{a}{r}\right)^2\right]}{\left(\frac{a}{b}\right)^2 + \left(\frac{b}{a}\right)^2}e^{-t/\tau} - \frac{\left[\left(\frac{r}{b}\right)^2 - \left(\frac{b}{r}\right)^2\right]}{2}\right\} \qquad (c)$$

where

$$\tau = \frac{\mu_o \sigma \Delta b}{2}\frac{\left[\left(\frac{b}{a}\right)^2 + \left(\frac{a}{b}\right)^2\right]}{\left[\left(\frac{a}{b}\right)^2 - \left(\frac{b}{a}\right)^2\right]} \qquad (d)$$

Show that the early and long-time responses do indeed match the results found in parts (a) and (b).

10.5.6 The configuration is as described in Prob. 10.4.5 except that the conducting shell is on the outside of the air gap at $r = a$, while the windings are on the inside surface of the air gap at $r = b$. Also, the windings are now arranged

so that the imposed surface current density is $\mathbf{K} = K_o(t)\sin\phi$. For this configuration, carry out parts (a), (b), and (c) of Prob. 10.4.5.

10.6 Magnetic Diffusion Laws

10.6.1* Consider a class of problems that are analogous to those described by (10.5.10) and (10.5.11), but with $\mathbf{J}$ rather than $\mathbf{H}$ written as a solution to the diffusion equation.

(a) Use (10.5.1)–(10.5.5) to show that

$$\nabla^2(\mathbf{J}/\sigma) = \mu\frac{\partial \mathbf{J}}{\partial t} \tag{a}$$

(b) Now consider $\mathbf{J}$ (rather than $\mathbf{H}$) to be z directed but independent of z, $\mathbf{J} = J_z(x,y,t)\mathbf{i_z}$, and $\mathbf{H}$ (rather than $\mathbf{J}$) to be transverse, $\mathbf{H} = H_x(x,y,t)\mathbf{i_x} + H_y(x,y,t)\mathbf{i_y}$. Show that

$$\nabla^2\left(\frac{J_z}{\sigma}\right) = \mu\frac{\partial J_z}{\partial t} \tag{b}$$

where $\mathbf{H}$ can be found from $\mathbf{J}$ using

$$\frac{\partial \mathbf{H}}{\partial t} = -\frac{\partial}{\partial y}\left(\frac{J_z}{\sigma\mu}\right)\mathbf{i_x} + \frac{\partial}{\partial x}\left(\frac{J_z}{\sigma\mu}\right)\mathbf{i_y} \tag{c}$$

Note that these expressions are of the same form as (10.5.8), (10.5.10), and (10.5.11), respectively, but with the roles of $\mathbf{J}$ and $\mathbf{H}$ reversed.

10.7 Magnetic Diffusion Step Response

10.7.1* In the configuration of Fig. 10.6.1, a steady state has been established with $K_s = K_p =$ constant. When $t = 0$, this driving current is suddenly turned off. Show that $\mathbf{H}$ and $\mathbf{J}$ are given by (10.6.21) and (10.6.22) with the first term in each omitted and the sign of the summation in each reversed.

10.7.2 Consider the configuration of Fig. 10.6.1 but with a perfectly conducting electrode in the plane $x = 0$ "shorting" the electrode at $y = 0$ to the one at $y = a$.

(a) A steady driving current has been established with $K_s = K_p =$ constant. What are the steady $\mathbf{H}$ and $\mathbf{J}$ in the conducting block?

(b) When $t = 0$, the driving current is suddenly turned off. Determine $\mathbf{H}$ and $\mathbf{J}$ for $t > 0$.

10.8 Skin Effect

10.8.1* For Example 10.7.1, the conducting block has length d in the z direction.

(a) Show that the impedance seen by the current source is

$$Z = \frac{a(1+j)}{d\sigma\delta}\frac{\left[e^{(1+j)b/\delta} + e^{-(1+j)b/\delta}\right]}{\left[e^{(1+j)b/\delta} - e^{-(1+j)b/\delta}\right]} \qquad (a)$$

(b) Show that in the limit where $b \ll \delta$, Z becomes the dc resistance $a/db\sigma$.

(c) Show that in the opposite extreme where $b \gg \delta$, so that the current is concentrated near the surface, the block impedance has resistive and inductive-reactive parts of equal magnitude and that the resistance is equivalent to that for a slab having thickness δ in the x direction carrying a current that is uniformly distributed with respect to x.

10.8.2 In the configuration of Example 10.7.1, the perfectly conducting electrodes are terminated by a perfectly conducting electrode in the plane $x = 0$.

(a) Determine the sinusoidal steady state response $\mathbf{H}$.

(b) Show that even though the current source is now "shorted" by perfectly conducting electrodes, the high-frequency field distribution is still given by (10.7.16), so that in this limit, the current still concentrates at the surface.

(c) Determine the impedance of a length d (in the z direction) of the block.